A STUDY OF ENERGY TRANSFER PROCESSES IN MOLECULAR LASERS

FINAL TECHNICAL REPORT

May 31, 1971

by

A.J. Glass, E.R. Fisher, R.H. Kummler, R. Marriott

Sponsored By

Advanced Research Projects Agency

ARPA Order No. 675, Am 7

Program Element Number 9E20

Principal Investigator: Dr. Alexander J. Glass
(313) 577-3864

Contractor: Wayne State University
Detroit, Michigan 48202

Contract Number: DAHC04-70-C-0022

Effective Date: 1/26/70

Expiration Date: 3/31/71

Amount: $30,100.00

Approved for public release: distribution unlimited

UNCLASSIFIED
Security Classification

DOCUMENT CONTROL DATA - R & D

(Security classification of title, body of abstract and indexing annotation must be entered when the overall report is classified)

1. ORIGINATING ACTIVITY *(Corporate author)*
Wayne State University
Detroit, Michigan 48202

2a. REPORT SECURITY CLASSIFICATION
UNCLASSIFIED

2b. GROUP

3. REPORT TITLE
A Study of Energy Transfer Processes in Molecular Lasers

4. DESCRIPTIVE NOTES *(Type of report and inclusive dates)*
Final Report (Technical) - 1/25/70 - 3/31/71

5. AUTHOR(S) *(First name, middle initial, last name)*
Alexander J. Glass , Edward R. Fisher, Ralph H. Kummler, Richard Marriott.

6. REPORT DATE	7a. TOTAL NO. OF PAGES	7b. NO. OF REFS
May 31, 1971	116	51

8a. CONTRACT OR GRANT NO.	9a. ORIGINATOR'S REPORT NUMBER(S)
DAHC04-70-C-0022	
b. PROJECT NO. ARPA Order No.675-Am 7	
c. Program Element No. 9E20	9b. OTHER REPORT NO(S) *(Any other numbers that may be assigned this report)*
d.	

10. DISTRIBUTION STATEMENT
Approved for public release; distribution unlimited.

11. SUPPLEMENTARY NOTES	12. SPONSORING MILITARY ACTIVITY
	U.S. Army Research Office Durham, North Carolina 27706

13. ABSTRACT

The Carbon Monoxide laser is one of the most promising systems currently available for the efficient generation of infrared radiation in the wavelength region from 5 to 8 um. A detailed model of the kinetic processes which govern the performance of this laser has been programmed for the IBM 360/67 computer. The temporal development of vibrational populations has been computed, and shown to converge to steady state solution generated elsewhere from algebraic computation. A careful investigation of scattering data shows an apparent discrepancy in the potential usdd to describe the interaction of the CO molecule with argon atoms. An experimental facility has been developed for observation of spontaneous emission from various molecular transitions in the CO laser.

DD FORM 1 NOV 68 1473 REPLACES DD FORM 1473, 1 JAN 64, WHICH IS OBSOLETE FOR ARMY USE.

UNCLASSIFIED
Security Classification

BLANK PAGE

A STUDY OF ENERGY TRANSFER PROCESSES IN MOLECULAR LASERS

FINAL TECHNICAL REPORT

May 31, 1971

by

A.J. Glass, E.R. Fisher, R.H. Kummler, R. Marriott

Sponsored By

Advanced Research Projects Agency
ARPA Order No. 675, Am 7
Program Element Number 9E20

Principal Investigator: Dr. Alexander J. Glass
(313) 577-3864

Contractor: Wayne State University
Detroit, Michigan 48202

Contract Number: DAHC04-70-C-0022

Effective Date: 1/26/70

Expiration Date: 3/31/71

Amount: $30,100.00

FOREWORD

This report is the final technical report on work carried out under Contract DAHC04-70-C-0022, which was administered by the U.S. Army Research Office, Durham. The findings in this report are not to be construed as an official Department of the Army position unless so designated by other authorized documents.

Abstract

The Carbon Monoxide laser is one of the most promising systems currently available for the efficient generation of infrared radiation in the wavelength region from 5 to 8 μm. A detailed model of the kinetic processes which govern the performance of this laser has been programmed for the IBM 360/67 computer. The temporal development of vibrational populations has been computed, and shown to converge to a steady state solution generated elsewhere from algebraic computation. A careful investigation of scattering data shows an apparent discrepancy in the potential used to describe the interaction of the CO molecule with Argon atoms. An experimental facility has been developed for observation of spontaneous emission from various molecular transitions in the CO laser.

Table of Contents

APPENDICES:

1. Vibration-Vibration Rate Coefficients
2. Fundamental Molecular Processes in Carbon Monoxide Laser Systems
3. The Vibrational Excitation of CO by Collision with Helium.

I. Introduction and Summary

A contract was awarded to Wayne State University for "A Study of Energy Transfer Processes in Molecular Lasers", with an effective starting date of 26 January, 1970. The effort under this contract is twofold. A computational effort is directed at modeling energy transfer processes important to molecular laser action using detailed computer codes, some of which were already in operation at Wayne State University. The experimental part of the effort, which is relatively small due to funding limitations, is directed at experimental verification of the computational and theoretical assumptions implicit in the calculational model. The principal investigator for this research is Dr. Alexander J. Glass, Professor of Electrical Engineering. Other faculty associates are Drs. Richard Marriott and Edward Fisher, Professors of Chemical Engineering. All three are members of the Research Institute for Engineering Sciences at Wayne State University.

I. 1 Description of the Model

Among the most important of the molecular laser systems currently in use is the CO laser. This laser operates between successive vibrational levels of the CO molecule, which is excited in an electrical discharge, either pulsed or CW, in the presence of He, N_2, and other additive gases, most usually O_2 and Xe. By varying the conditions of excitation, the gas mixture, and the dispersive properties of the laser cavity, various ($\Delta v = 1$) vibrational transitions can be stimulated, giving the CO laser a wavelength diversity far greater than other molecular lasers. As examples of the variation in output which can be achieved in the CO laser, the range of operating wavelengths which have been observed at room temperature, with CW oscillation, by Bhaumik and co-workers[1] as shown in Table I - 1. Similarly, in Table I - 2, we show the range of transitions observed with pulsed excitation,

at 77°K, by Graham et al.[2]. It is the main purpose of the research outlined in this report, to develop a model for the CO laser system which is of sufficient flexibility to provide a sound analytic basis for determining the optimum operating conditions for the CO laser, for either pulsed or CW operation, at any wavelength in the range of operation.

Stimulated emission in any laser system is the result of the creation of an inverted population[3], a condition in which the population of a given excited quantum state exceeds that of a quantum state of lower energy (barring degeneracies). In order to achieve inversion in the CO system, several different energy transfer processes must play a role. To begin with, excitation of the CO molecules by impact with energetic electrons in the discharge must take place. As is shown in Chapter III of this report, there are no selective excitation processes taking place in the CO laser, at least not to any great degree, so that from excitation rates only, we would not expect to find an inversion of population. It is not until we consider the effect of vibrational energy transfer (V - V) that the inversion mechanism becomes clear. In an anharmonic system like CO, providing that the average kinetic energy of the molecules is kept well below the vibrational level separation, a significant deviation from a Boltzmann distribution of vibrational populations can be created, with an accumulation of population in the higher lying states[4]. Detailed calculations of this effect are exhibited in Chapter III of this report. In order to assure that the gas temperature remains low, helium is added to the discharge, to provide good heat conduction to the walls. Thus the model must include electron excitation of vibrational states, V - V and V - T processes among the molecular species present in the laser, and the effect of neutral atom collisions with the molecules. Each of these processes is characterized by a cross section, which depends on the relative

velocity of the collision partners. These cross sections must be integrated over the appropriate velocity distributions to obtain the rate coefficients for the respective processes. It is assumed in this research that the kinetic energy distributions of the atomic and molecular constituents of the gas are characterized by a single gas temperature, and are described by a Maxwell-Boltzmann distribution of velocities. The vibrational levels are treated explicitly, by a set of coupled rate equations for the vibrational populations, the master equation. The electronic velocity distributions are assumed to be Maxwellian, at a temperature different from the gas temperature. It has been shown[5] that in a weakly ionized, molecular plasma, the electron velocity distribution deviates from Maxwellian form, but, as is discussed in Chapter III, this deviation has little effect on the vibrational excitation rate coefficients.

Radiation processes must also be considered in the model. Only spontaneous emission has been treated to date, so the model only applies to laser performance below and up to the threshold of oscillation. This is sufficient for comparison with observation, however, since the principal diagnostic measurement is spontaneous emission from the various levels in the discharge (sidelight emission).

I. 2 Summary of the Report and Results

Chapter II of the report considers the vibrational excitation of carbon monoxide by collisions with inert gas atoms, in particular, argon and helium. In both cases, experimental data on vibrational relaxation of CO in the presence of the atomic gas are available, for comparison to the calculated values. A detailed description is given of the close coupling calculation. It is necessary in this calculation to represent the atom-molecule interaction by some potential function of the separation coordinate. At first, the Lennard-Jones (6 - 12) potential[6] was employed.

The computed relaxation times were smaller, by significant factors, than experimental data, both for He-CO, Ne-CO and Ar-CO. In order to determine the cause of this discrepancy, the calculations were repeated using an empirical, "soft-core" potential[7], obtained from scattering data. Using the modified potentials, satisfactory agreement with experiment was obtained for CO-He mixtures, but for CO-Ar mixtures, the calculated relaxation times exceeded the experimental values by a factor of 50. This unexpected disagreement may be due to the presence of quenching impurities, such as H_2O, or H_2, in the experiment, but it is felt that this is unlikely. The exact cause of the discrepancy remains unresolved at present.

In Chapter III, a detailed summary is given of the computational approach employed in the solution of the master equation. Up to 30 vibrational levels of both N_2 and CO, or indeed any pair of diatomic gases, can be explicitly included, along with electrons and inert atoms. A preliminary test of the code was performed by considering the reaction of vibrationally excited H_2 and D_2 to form HD in the absence of electrons. Detailed comparisons are given for the Raman excitation of the vibrational levels of H_2 in the presence of D_2, as carried out by Bauer et al.[8]. Good agreement with experiment is obtained. It is also pointed out that a more definitive reaction in order to test the proposed HD mechanism would proceed from the excitation of D_2 in the presence of H_2. To date, the latter experiment has not been carried out.

The dependence of the vibrational excitation rates on electron temperature is then discussed. It is found that the excitation rates are insensitive to the shape of the high energy tail of the electron distribution $T_e \geq 10000^\circ K$ for vibrational excitation. Accordingly, a Maxwellian distribution can be used to describe the electron distribution in the model. Finally, the transient response of the CO-N_2 laser mixture to an initially established electron temperature is computed, and is shown to converge in time to the steady-state results of Rich[9].

In Chapter IV, a brief discription is given of the experimental facility. There are three appendices to the report, a discussion of the calculation of V - V rate coefficients, a summary of the modeling calculations, which was presented at the Conference on Laser Physics at Sun Valley, Idaho, on March 1 - 3, 1971, by Drs. Fisher and Kummler, and a discussion of the vibrational excitation of CO by collision with He, a paper to be given at VII International Conference on the Physics of Electronic and Atomic Collisions, by Dr. Marriott.

TABLE I - 1

Spectral Output of CO Laser at 20°C(μm)

λ Observed (Air)	λ Theoretical (Air)	ν cm^{-1}	Vibrational Band	Transition	Relative Intensity
5.3155	5.3152	1880.897	8 - 7	P(20)	80
5.3275	5.3273	1876.629		P(21)	9
5.3397	5.3395	1872.329		P(22)	10
5.3871	5.3876	1855.615	9 - 8	P(20)	100
5.3993	5.3999	1851.382		P(21)	16
		1842.821	10 - 9	P(17)	
5.4487	5.4494	1834.577		P(19)	52
5.5131	5.5127	1813.514	11 - 10	P(18)	17
5.5256	5.5252	1089.416		P(19)	1.8
5.5901	5.5901	1788.398	12 - 11	P(18)	2.2
5.6027	5.6028	1784.334		P(19)	0.9
5.6559	5.6567	1767.359	13 - 12	P(17)	0.3
5.6688	5.6695	1763.363		P(18)	0.5
5.6819	5.6825	1759.334		P(19)	----
5.6991	5.6996	1754.060	14 - 13	P(14)	0.3

TABLE I - 2. Partial Summary of Observations at 77°K for 0.3 Torr CO Plus 5 Torr Helium.

Observed Transitions		Strongest Line Data				
v → v'	P(J) [a]	J	λ vac (microns)	Current (Amp)	Laser Output (watts)	Laser Pulse (msec)
4 → 3	5 - 8	7	4.90882	0.198	1.2	0.2
5 → 4	5 - 8	7	4.97283	0.193	0.68	0.3
6 → 5	5 - 8	7	5.03735	0.193	0.40	0.3
7 → 6	5 - 8	8	5.11437	0.335	0.47	0.4
8 → 7	5 - 8	7	5.17189	0.285	0.12	0.1
9 → 8	6	6	5.23190	0.213	0.005	0.3
10 → 9	7	7	5.31342	0.713	0.007	5.0

[a] Includes only those transitions for which laser power exceeded 1 mw.

References to Chapter I

1. M.L. Bhaumik, W.B. Lacina, and M.M. Mann, IEEE Journal of Quantum Electronics 7, (June 1971). To be published.

2. W.J. Graham, J. Kershenstein, J.T. Jensen, and K. Kerhenstein, Appl. Phys. Letters 17, 194 (1970).

3. A.L. Schawlow and C.H. Townes, Phys. Rev. 112, 1940 (1958).

4. E.R. Fisher and R.H. Kummler, J. Chem. Phys. 49, 1075 and 1085 (1968).

5. W. Nighan and J.H. Bennett, Appl. Phys. Letters 14, 240 (1969).

6. J.O. Hirschfelder, F.C. Curtiss, R.B. Bird, Molecular Theory of Gases and Liquids, John Wiley, New York (1954).

7. F. Amdur, E.A. Mason, and J.E. Jordan, J. Chem. Phys. 27, 527 (1957).

8. S.H. Bauer, Private Communication.

9. J.W. Rich, Appl. Optics, (1971) in press.

II. A THEORETICAL STUDY OF THE VIBRATIONAL EXCITATION OF CARBON MONOXIDE BY INERT GAS COLLISIONS

1. Introduction

Inelastic processes involving the vibrational excitation of molecules by collision with inert gases are of particular relevance to the study of gas laser phenomena. Much of the necessary data is not available. Direct experimental measurements of the corresponding low energy collision cross sections have not been made and the non Boltzmann nature of the system may well render invalid any extrapolation based on laboratory observation of vibrational relaxation processes. It is of importance, therefore, to establish the quantitative reliability of the theoretical procedures for calculating the rate processes required.

In previous publications (Marriott[1],[2], Gianturco and Marriott [3]) a method for the close coupling calculation of cross sections for the vibrational excitation of molecules by collision with atomic particles has been developed and applied to a variety of collision processes.

In this report the method is applied to the vibrational excitation of CO by collision with Ar and He. There are no anomalous features in the interactions between the particles in either case, consequently the results obtained would be expected to be as reliable as those obtained in the original study of CO - CO collisions (Gianturco and Marriott[3]). Experimental data is available on the vibrational relaxation of the mixtures (Hooker[4], Millikan[5]) for comparison with the calculations.

As summarized in section 2, the close coupling calculation is based upon the assumption of a spherically symmetric semi-empirical scattering potential. However, it is found that use of the appropriate Lennard-Jones potential as was done in the original calculations, leads to vibrational relaxation times that are too short, hence by inference to cross sections for the excitation of the first vibrational level of CO that are too large. The details of these calculations, including the result for a similar CO-Ne calculation, are presented in sections 3, 4 and 5. Sections 6 and 7 present a recalculation of the cross sections for excitation by Ar and He based upon the more realistic short range potentials measured by Amdur et al.[6] and Jordan et al.[7] for collision energies up to 2.5 eV. This leads to satisfactory agreement with experimental relaxation times for the case of CO-He mixtures. However, for the CO-Ar system it is found that the calculated relaxation times are now greater than experiment by about a factor of 50.

This surprising disagreement, occuring in what would have been expected to be a routine calculation, is investigated in detail in section 8. The theoretical results are confirmed. At the same time it is estimated that the degree of contamination of Ar by H_2 or H_2O which could account for an experimental error of this size, though small would still be two orders of magnitude larger than is normal. The disagreement remains unresolved.

2. Collision theory

In summary, the analysis of the collision process neglects the effects of the rotational states of the target and the internal structure of the impacting particle. It assumes the molecular wave function to be separable into electronic, rotational and vibrational components and the scattering potential to be similarly separable in terms of the molecular normal coordinates and to be spherically symmetric.

To this approximation the coupled radial scattering equations take the form using atomic units throughout,

$$\left[\frac{d^2}{dr^2} + k_n^2 - \frac{\ell(\ell+1)}{r^2}\right]F_n^\ell(r) = 2M\sum_{m=0}^{\infty} F_m^\ell(r)\, V_{nm}^\ell(r) \qquad (1)$$

where the wave number of the scattered particle of reduced mass M is given by

$$k_n^2 = 2M(E_p - E_n + k_p^2/2M) \qquad (2)$$

E_n being the energy of the nth molecular vibrational state and the initial state being arbitrarily assigned the subscript p.

The scattering equations (1) are solved numerically with the retention of all coupling between any specified set of molecular states subject to the boundary conditions

$$F_n^\ell(0) = 0 \qquad (3)$$

$$F_n^\ell(r) \sim i^\ell(2\ell+1)\left[\delta_{pn}k_p^{-1}\sin(k_p r - \ell\pi/2) + \exp(ik_n r - i\ell\pi/2)\, f_{pn}^\ell\right]$$

The corresponding inelastic partial cross sections for the collision induced transitions are then given by

$$Q_{pn}^{\ell} = 4\pi \frac{k_n}{k_p} (2\ell+1) |f_{pn}^{\ell}|^2 \qquad (4)$$

and the total cross sections obtained by graphical integration over all significant values of ℓ.

The transition matrix elements for a diatomic molecule are shown to be approximated by

$$V_{nm}^{\ell}(r) = V_o V(r) V_{nm}^{\ell} \qquad (5)$$

where numerical values for the V_{nm}^{ℓ} factors are estimated in the usual way from the classical distance of closest approach of the colliding particles (Marriott [2]).

Empirical functions are employed to represent the scattering potential component, V(r), and the normalising constant V_0 is taken to be $(V_{00}^{\ell})^{-1}$. This ensures that the scattering potential for the ground state molecule is given by the observed empirical function.

This close coupling analysis of the collision process has been programmed in Fortran for the IBM 360 series computer.

3. The Lennard-Jones intermolecular potential

Previous calculations for collision systems involving CO have successfully employed the semi-empirical Lennard-Jones functions to represent the scattering potential between the CO and the impacting particle (Gianturco and Marriott [3]).

To this approximation the potential is given by a function of the form

$$V(r) = 4\varepsilon\left[\left(\frac{\sigma}{r}\right)^{12} - \left(\frac{\sigma}{r}\right)^{6}\right]$$

where the necessary parameters can be estimated using the combination rules for non polar mixtures discussed by Hirschfelder et al.[8]

$$\varepsilon_{mix} = (\varepsilon_{CO}\varepsilon_{X})^{\frac{1}{2}}, \quad \sigma_{mix} = \tfrac{1}{2}(\sigma_{CO} + \sigma_{X})$$

Hirschfelder et al. give for the component parameters:

$\varepsilon_{CO}/k = 88^{o}K$ $\qquad$ $\sigma_{CO} = 3.706 \times 10^{-8}$cm

$\varepsilon_{Ar}/k = 116^{o}K$ $\qquad$ $\sigma_{Ar} = 3.465 \times 10^{-8}$cm

$\varepsilon_{Ne}/k = 27.5^{o}K$ $\qquad$ $\sigma_{Ne} = 2.858 \times 10^{-8}$cm

$\varepsilon_{He}/k = 10.2^{o}K$ $\qquad$ $\sigma_{He} = 2.556 \times 10^{-8}$cm

k being the Boltzmann constant, and these lead in turn to the values for the mixtures:

CO + Ar : $\varepsilon = .320 \times 10^{-3}$ a.u., $\sigma = 6.79\ (a_0)$

CO + Ne : $\varepsilon = .156 \times 10^{-3}$ a.u., $\sigma = 6.22\ (a_0)$

CO + He : $\varepsilon = .950 \times 10^{-4}$ a.u., $\sigma = 5.93\ (a_0)$

A typical matrix of transition elements obtained for the CO + Ar system at several collision energies and an impact parameter of zero are shown in table 1.

Table 1. Matrix elements for head-on collision of Ar with CO assuming a Lennard-Jones interaction.

	Collision Energy (eV)+	0.6	1.0	1.5	2.0	2.5
Transition elements*	V_{00}	1.0000	1.0000	1.0000	1.0000	1.0000
	V_{10}	0.0777	0.0801	0.0820	0.0834	0.0846
	V_{11}	1.0060	1.0064	1.0067	1.0070	1.0072
	V_{20}	0.0043	0.0045	0.0048	0.0049	0.0051
	V_{21}	0.1102	0.1137	0.1164	0.1184	0.1200
	V_{22}	1.0121	1.0129	1.0135	1.0140	1.0143
	V_{30}	0.0002	0.0002	0.0002	0.0002	0.0002
	V_{31}	0.0074	0.0079	0.0083	0.0085	0.0088
	V_{32}	0.1345	0.1396	0.1430	0.1455	0.1475
	V_{33}	1.0182	1.0193	1.0203	1.0210	1.0215

+Relative to ground state

*V_{00} nomalized to 1.0

4. Vibrational excitation cross sections (LJ)

Using the Lennard-Jones potential described in the previous section the remaining parameters required as data for the computer code are the reduced oscillator mass (0.126×10^5 atomic units), the vibrator energy level separation for CO (0.266 eV) and the collision reduced masses:

$$CO + Ar;\ .3024 \times 10^5 \text{ a.u.},\ CO + Ne;\ .2149 \times 10^5 \text{ a.u.},$$
$$CO + He;\ .6433 \times 10^4 \text{ a.u.}$$

The calculated partial sections for the excitation of the first vibrational state by Ar are shown in figure 1 where coupling between the first four states has been retained and in figure 2 where coupling has been restricted to the first two states. The total cross sections, obtained by graphical integration of these figures are presented as functions of collision energy in table 2.

An indication of the numerical accuracy attained was given by the fact that detailed balance held in all cases to at least 3 significant figures. Inclusion of more than four vibrational states was not found to have any further significant effect on the Q_{01} cross section.

The results for the Ne and He calculations were quite similar in form to those for Ar and the details are not included here.

Cross sections for the excitation of CO from the ground to the first vibrational level in the three collision systems are shown in table 3. In these calculations coupling has been retained between the first 3 or 4 vibrational state of CO.

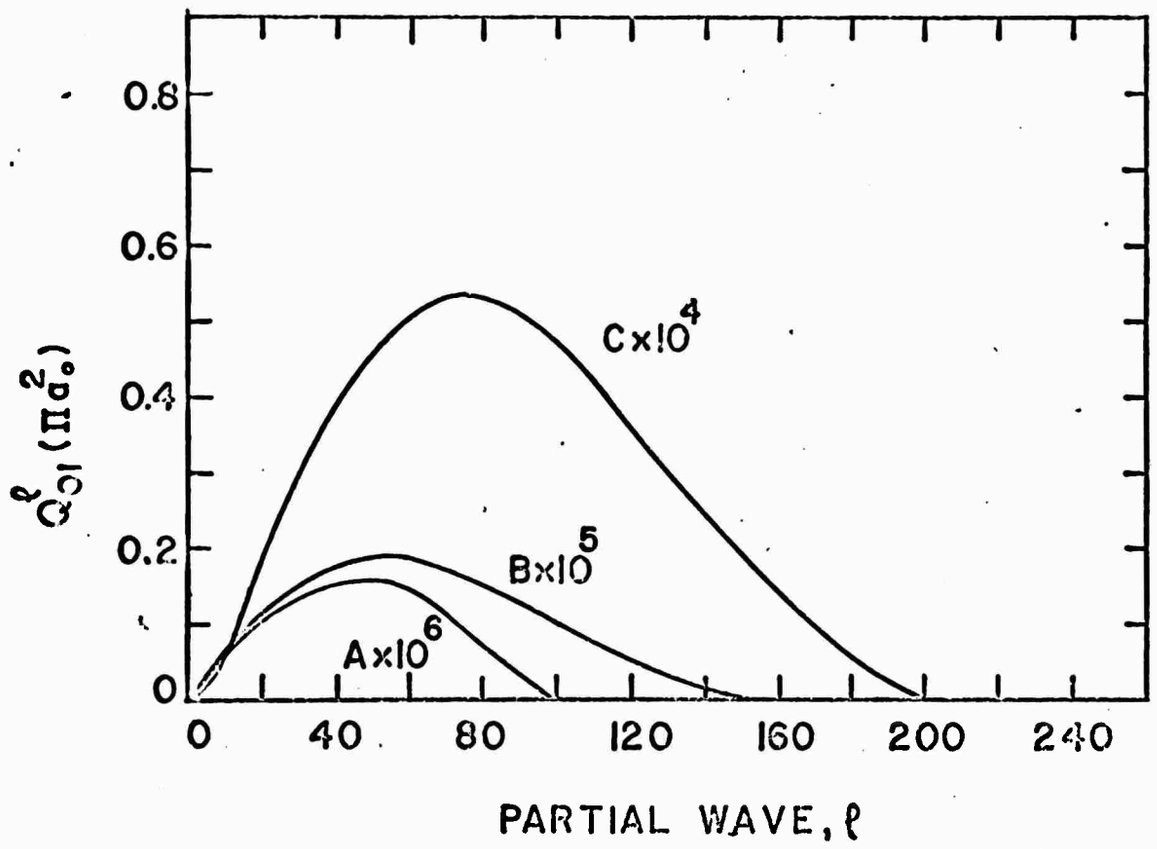

Figure 1. Calculated partial cross sections for the excitation of the first vibrational level of CO by collision with Ar for a Lennard-Jones interaction at several collision energies and including coupling between the first four vibrational states.
A, collision energy 0.8 eV; B, collision energy 1.0 eV; C, collision energy 1.5 eV.

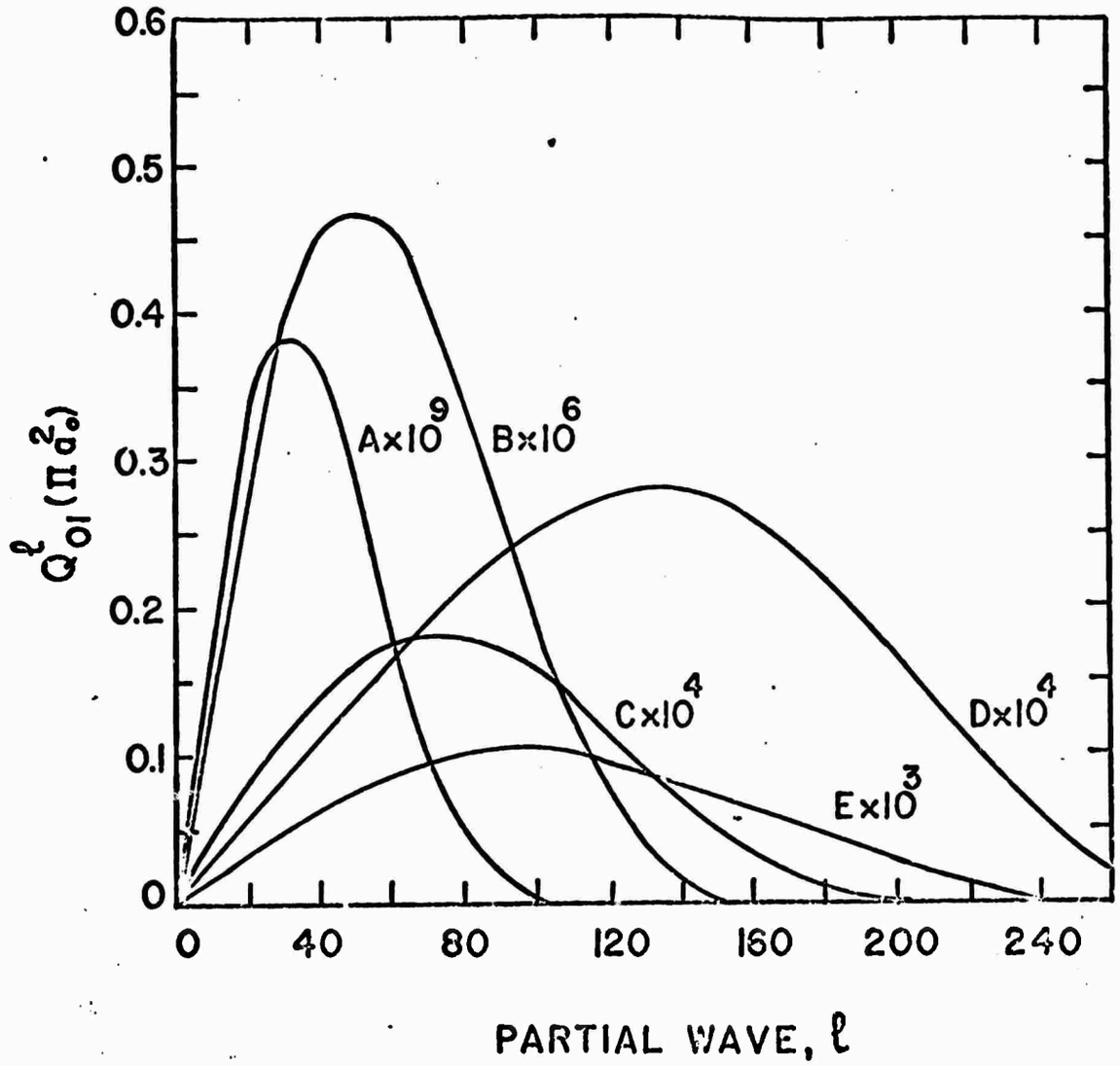

Figure 2. Calculated partial cross sections for the excitation of the first vibrational level of CO by collision with Ar for a Lennard-Jones interaction at several collision energies and including coupling between the first two molecular vibrational states A, collision energy 0.6 eV; B, collision energy 1.0 eV; C, collision energy 1.5 eV; D, collision energy 2.0 eV; E, collision energy 2.5 eV.

Table 2. Total cross sections for vibrational excitation of CO by Ar impact assuming a Lennard-Jones interaction potential.

Collision energy (eV)	Two coupled states $Q_{01}(\pi a_o^2)$	Four coupled states $Q_{01}(\pi a_o^2)$
0.266	0.00	0.00
0.6	0.20^{-7*}	----
0.8	----	0.98^{-5}
1.0	0.35^{-4}	0.16^{-3}
1.5	0.20^{-2}	0.57^{-2}
2.0	0.14^{-2}	----
2.5	0.42^{-1}	----

Table 3. Total cross sections (LJ) for the vibrational excitation of CO from the ground to the first excited level by collision with Ar, Ne and He.

Collision energy (eV)		0.6	0.8	1.0	1.5	2.0
Helium	$Q_{01}(\pi a_o^2)$	$.16^{-1*}$	$.84^{-1}$	.24	.97	$.19^{+1}$
Neon	$Q_{01}(\pi a_o^2)$	$.24^{-4}$	$.55^{-3}$	$.39^{-2}$	$.66^{-1}$	.30
Argon	$Q_{01}(\pi a_o^2)$	-	$.98^{-5}$	$.16^{-3}$	$.57^{-2}$	-

* superscript denotes the power of 10 by which the number must be multiplied.

5. Vibrational relaxation of CO in the inert gases

No direct measurements of vibrational excitation cross sections for heavy particle collisions have yet been made. Comparison of theory with experiment can only be obtained in an indirect way by using the cross sections to determine the relaxation time for CO in the corresponding gas. These relaxation times may then be compared with the experimental results of Hooker and Millikan[4] and Millikan[5].

The connection between the relaxation time, τ, for a simple harmonic vibrator and the corresponding process reaction rate coefficient, γ_{nm}, has been discussed by Herzfeld and Litovitz[9].

If it is assumed that vibrational transitions can occur only to neighboring states, then it can be shown that, for a diatomic gas in translational equilibrium

$$1/\tau = \gamma_{10} - \gamma_{01} \tag{6}$$

where in general for a gas mixture of C components of fractional molecular concentrations χ_i

$$\gamma_{nm} = \sum_{i=1}^{C} \chi_i \, \gamma_{nm}^i \tag{7}$$

where

$$\gamma_{nm}^i = 4\pi N \left(\frac{M_i}{2\pi kT}\right)^{3/2} g_m \int_0^\infty Q_{nm}^i(v) \exp(-M_i v^2/2kT) v^3 dv$$

N being the number density of the gas, g_m the statistical weight of the m vibrational state, M_i the reduced mass for the molecular vibrator and the i'th mixture component and the $Q_{nm}^i(v)$ the cross section for the n→m transition induced by collision at velocity v with the i'th mixture component. For

the reverse reaction, detailed balancing gives immediately

$$\gamma_{mn} g_m \exp(-E_m/kT) = \gamma_{nm} g_n \exp(-E_n/kT).$$

The relative magnitudes of the transition elements in table 1 indicate that, as was the case for pure CO, the assumption that only single quantum jump transitions can occur should be valid to a good approximation for CO in Ar. A similar conclusion is reached for the other inert gases.

The relaxation time for CO in Ar obtained on this basis by the numerical integration of equation (7) using the excitation cross sections in table 3 and taking N to be the particle density for 1 atmosphere pressure at T°K, is shown as a function of temperature in figure 3. Substitution of the parametric values for the CO-Ar system reduces equation (7) to the convenient form

$$\gamma_{nm} = \frac{2.303 \times 10^9}{T^{\frac{1}{2}}} \int Q_{nm}(E) \exp(-E/kT) (E/kT) d(E/kT) \quad \text{sec}^{-1} \text{ atm.} \tag{8}$$

where Q_{nm} is in units of πa_o^2.

The experimental results of Hooker and Millikan are also shown in figure 3. It is immediately apparent that the theoretical relaxation time is consistently smaller than the observed value by a factor of four. This in turn implies that the calculated cross sections for the excitation of the first vibrational level of CO by collision with Ar are too large by the same factor.

For the relaxation of CO in He the required rate coefficient, in the same notation, is given by

$$\gamma_{01} = 4(10)^{11} (MT)^{-\frac{1}{2}} \int_0^\infty Q_{01}(E) (E/kT) e^{-E/kT} d(E/kT) \quad \text{sec}^{-1} \text{ atm.} \tag{9}$$

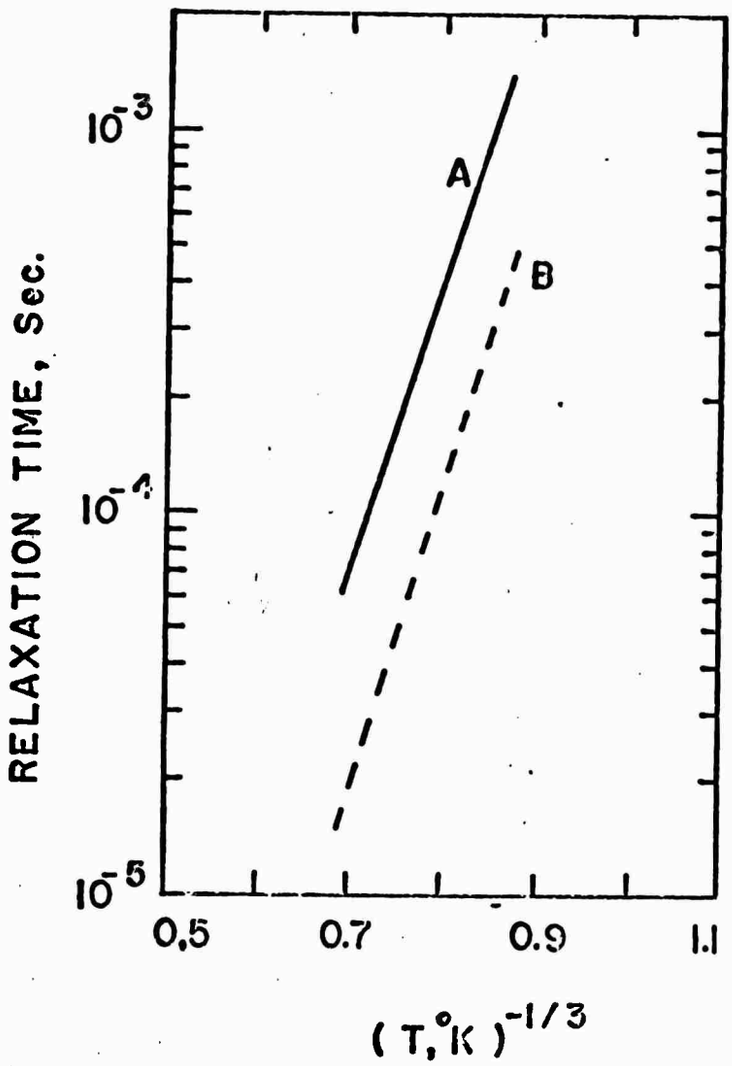

Figure 3. Vibrational relaxation time for CO in Ar at one atmosphere pressure.

A. Experimental results of Hooker and Millikan[4].

B. Calculated in this paper using a Lennard-Jones scattering potential with coupling between the first four vibrational states.

The theoretical relaxation times for CO in He obtained in this way are shown in figure 4 in comparison with the experimental values. It is again apparent that theory is consistently less than experiment, now by a factor of fifty.

A similar result is obtained for CO in Ne which is intermediate between those for Ar and He. The theoretical relaxation time for the Ne mixture is found to be low by a factor of seven.

In view of the excellent agreement between theory and experiment for the case of pure CO (Gianturco and Marriott [3]) these discrepancies appear to be significant.

It is of importance, therefore, to establish where the approximations that proved satisfactory in the treatment of CO-CO collisions fail for the similarly weakly interacting inert gas systems. Evidently the part of the present calculation that involves greater approximation than was the case for pure CO is the specification of the scattering potential itself.

Taken together the results indicate that the repulsive core of the Lennard-Jones potential, which dominates the vibrational excitation process, seriously overestimates the strength of the short range interaction between CO and the inert gases.

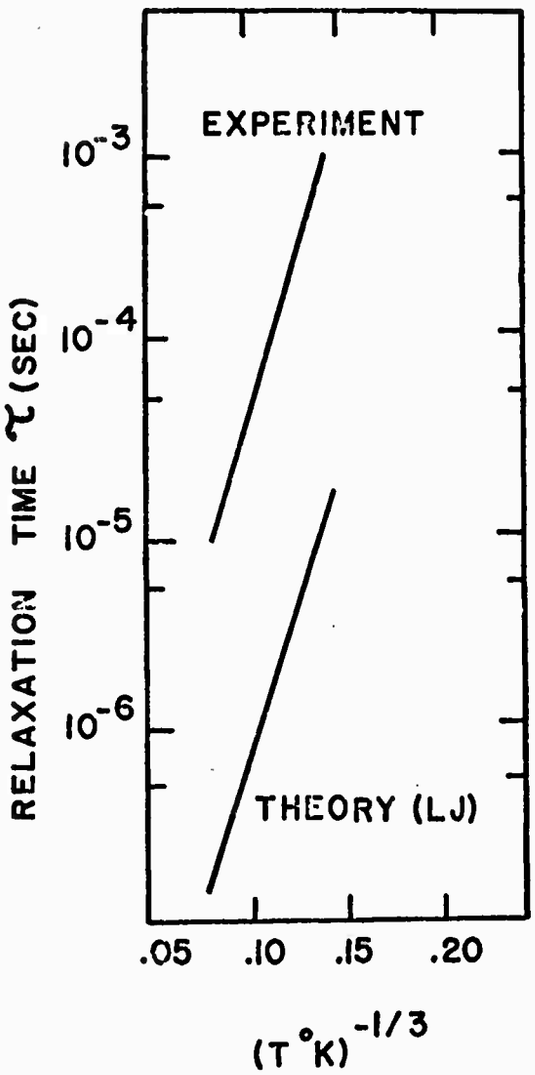

Figure 4. Vibrational relaxation time for CO in He at one atmosphere pressure. Experimental results of Millikan [5]. Theory (LJ); calculated in this paper using a Lennard-Jones potential with coupling between up to 4 vibrational states.

6. The soft core intermolecular potential

The scattering studies by Amdur et al. [6] and Jordan et al. [7] of a number of gas molecule potentials indicate that the repulsive part of the interaction between CO and the inert gases behaves as r^{-7} rather than r^{-12}. This represents a much softer interaction than the Lennard-Jones core, which behaves as r^{-12}, and thus it follows that use of the Lennard-Jones potential will yield cross sections that are too large.

For the CO-Ar interaction the soft core potential is given in the form

$$V(r) = 47529/r^{6.99} \qquad (10)$$

for particle separation in the range

$$3.8 \leq r(a_o) \leq 5.$$

Since no experimental information is available for separations greater than this it is assumed in the following calculations that the Lennard-Jones potential discussed in Section 3 can be used to represent both the long range interaction outside the potential minimum and also the location of the potential zero.

Subject to these restrictions a polynomial fit was constructed which smoothly joined the short range soft core to the long range Lennard-Jones function.

The specific analytic expression used was

$$V(r) = .0422(\sigma - r) + .0684(\sigma - r)^2 + .0422(\sigma - r)^3 + .00692(\sigma - r)^4 \quad (eV) \qquad (11)$$

where

$$5 \leq r(a_o) \leq 7.5$$

and σ is the appropriate Lennard-Jones parameter.

For separations $r(a_o) > 7.5$ the Lennard-Jones function described in Section 2 was used.

Figure 5 shows schematically the complete function. Clearly this potential cannot be validly employed for collision energies greater than 4.2 eV. However, this is considerably higher than the energies of interest here.

The matrix of transition elements obtained on the basis of this potential at several collision energies and zero impact parameter are shown in table 4.

Comparison of table 4 with table 1 shows immediately that for the soft core potential, as for the Lennard-Jones, transitions from the ground to the first excited vibrational level would be expected to dominate the vibrational relaxation process. In addition corresponding V_{10} matrix elements are now smaller by a factor of about 2.

For the CO-He system the interaction has not been measured directly. However, data is given on the N_2- He system, and it is shown that the CO and N_2 interactions are very similar.

On this basis we estimate the repulsive interaction for CO-He to be $232/r^7$(a.u.) for separations $3 < r(a_o) < 4.3$. For the long range part the Lennard-Jones potential is assumed still valid and the two functions are smoothly joined over a small region by the commone tangent:

$$V(r) = .04739 - .009158r \text{ for } 4.53 < r(a_c) < 4.84.$$

Use of this soft core (SC) potential again reduces the strength of the coupling between vibrational states by about a factor of 2 as was the case for the CO-Ar soft core potential. This reduction in magnitude of the coupling terms would be expected to lead in turn to a reduction in magnitude of the cross sections.

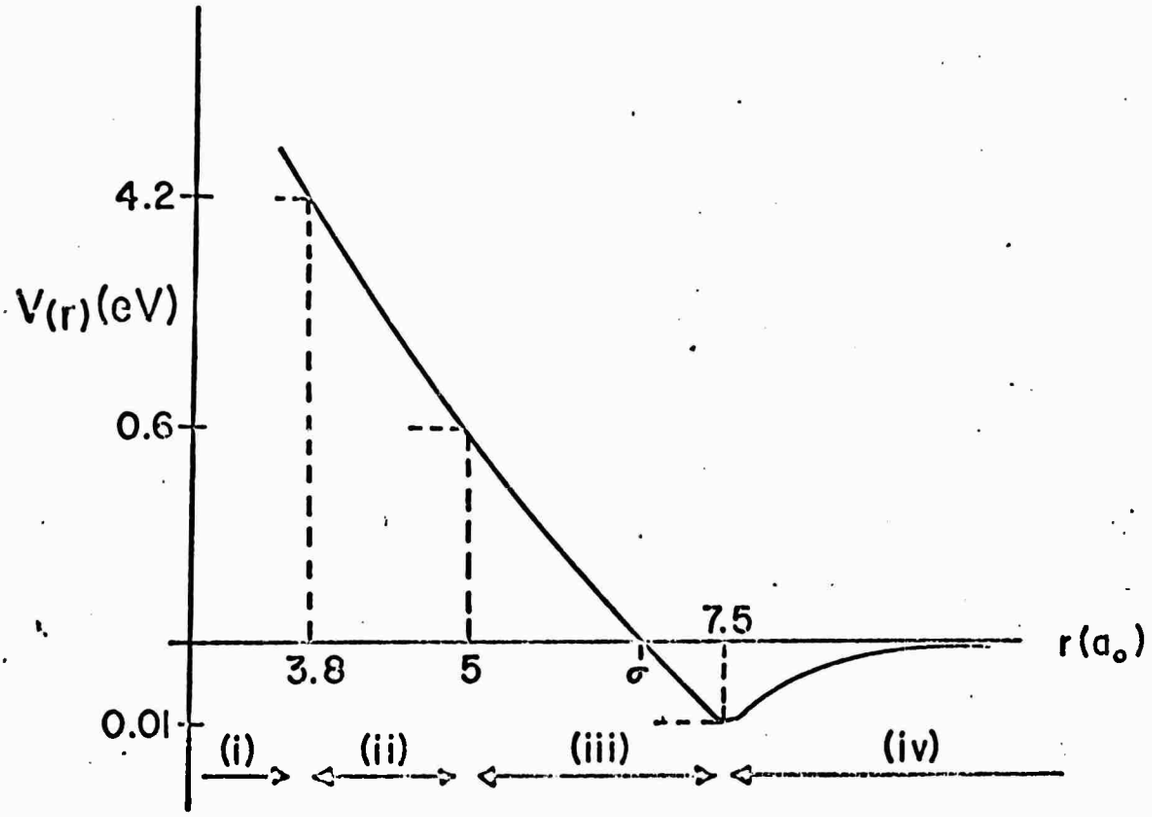

Figure 5. Empirical soft core CO-Ar interaction potential

Region (i) Potential undefined

Region (ii) Empirical potential after Jordan et al.[7]

Region (iii) Polynomial fit

Region (iv) Lennard-Jones after Hirschfelder et al.[8]

Table 4. Transition elements for head on collision of Ar with CO and the soft core interaction.

Collision Energy (eV)+		0.6	1.0	1.5	2.0	2.5
Transition elements*	V_{00}	1.0000	1.0000	1.0000	1.0000	1.0000
	V_{10}	.0421	.0460	.0493	.0517	.0535
	V_{11}	1.0018	1.0021	1.0024	1.0027	1.0029
	V_{20}	.0013	.0015	.0017	.0019	.0020
	V_{21}	.0596	.0651	.0698	.0732	.0758
	V_{22}	1.0035	1.0042	1.0049	1.0057	1.0057
	V_{30}	.0000	.0000	.0000	.0001	.0001
	V_{31}	.0022	.0026	.0030	.0033	.0035
	V_{32}	.0730	.0798	.0856	.0897	.0930
	V_{33}	1.0053	1.0064	1.0073	1.0080	1.0086

+ Relative to ground state

* V_{00} normalized to 1.0

7. Excitation cross sections (SC) for CO collision with Ar and He

The partial cross sections for CO-Ar collisions calculated on the basis of the corresponding soft core potential described in the previous section and the remaining collision parameters listed in section 3 are shown in figures 6 and 7. The total cross sections obtained by graphical integration of the curves for the case of two and three coupled vibrational states are shown in table 5 together with the corresponding Lennard-Jones cross sections for excitation from the ground to the first vibrational level for comparison.

As expected the (SC) cross sections are smaller than their corresponding counterparts by about a factor of 2 at low energies. However, this difference increases with energy, being about an order of magnitude at 1 eV and rising to a factor of 50 at 2.5 eV.

The divergence between the (SC) and (LJ) cross sections increases with collision energy as a consequence of the rapid increase of the difference between the potential functions as the classical distance of closest approach decreases.

The results of the CO-He calculation were quite similar in form to those for Ar although larger by orders of magnitude, and are not presented in detail here. The total cross sections obtained for the CO-He system are shown in table 6, once again with the corresponding Lennard-Jones results for comparison. The numerical convergence of these He cross sections was confirmed by retaining coupling between up to six vibrational states. Overall numerical accuracy was indicated as previously by the fact that detailed balance was satisfied throughout to 3 significant figures.

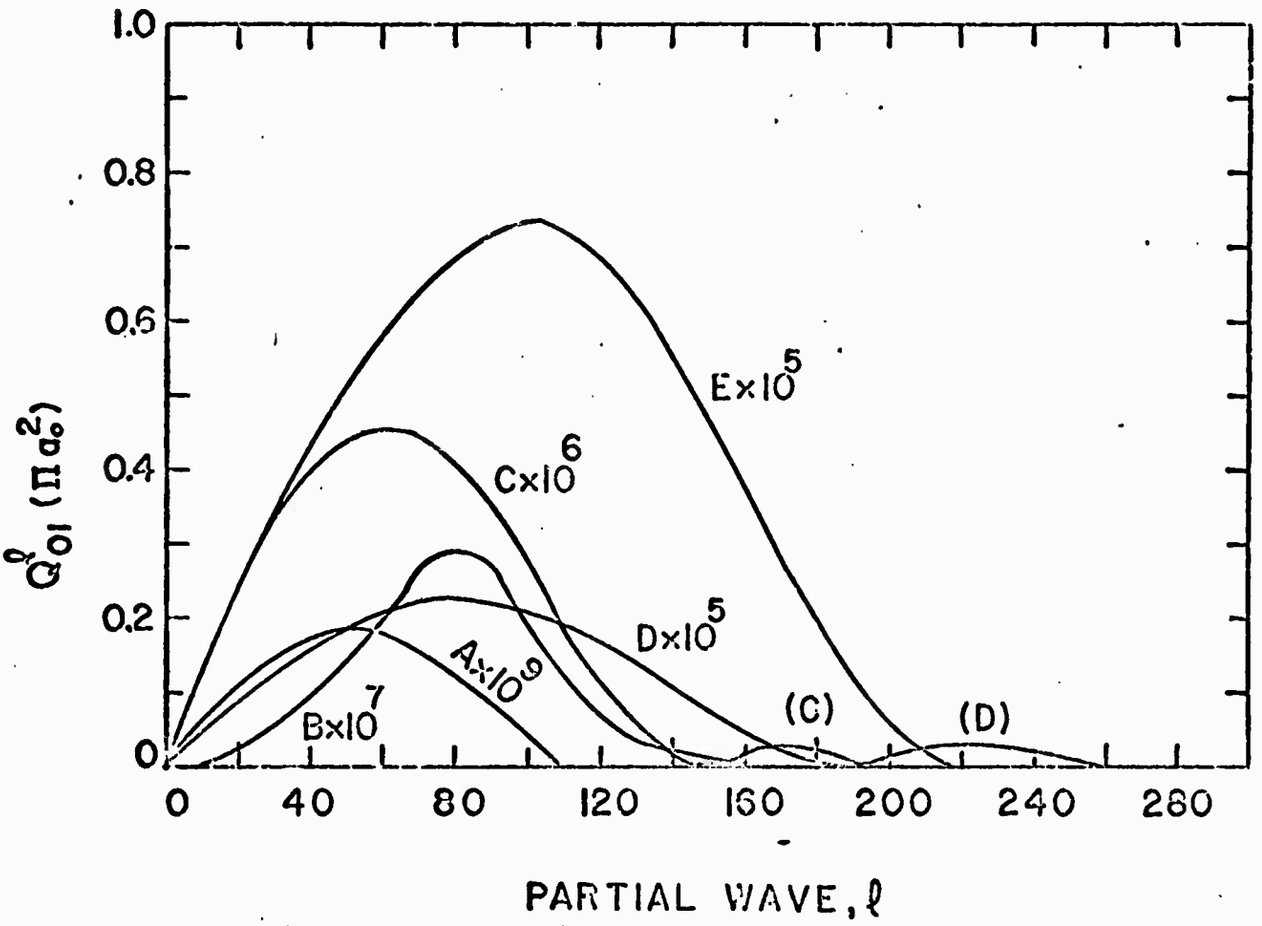

Figure 6. Partial cross sections for the excitation of CO from the ground to the first vibrational level by Ar impact, calculated at several collision energies assuming a soft core scattering potential and with coupling retained between the first two vibrational states. A, 0.6 eV; B, 1.0 eV; C, 1.5 eV; D, 210 eV; E, 2.5 eV.

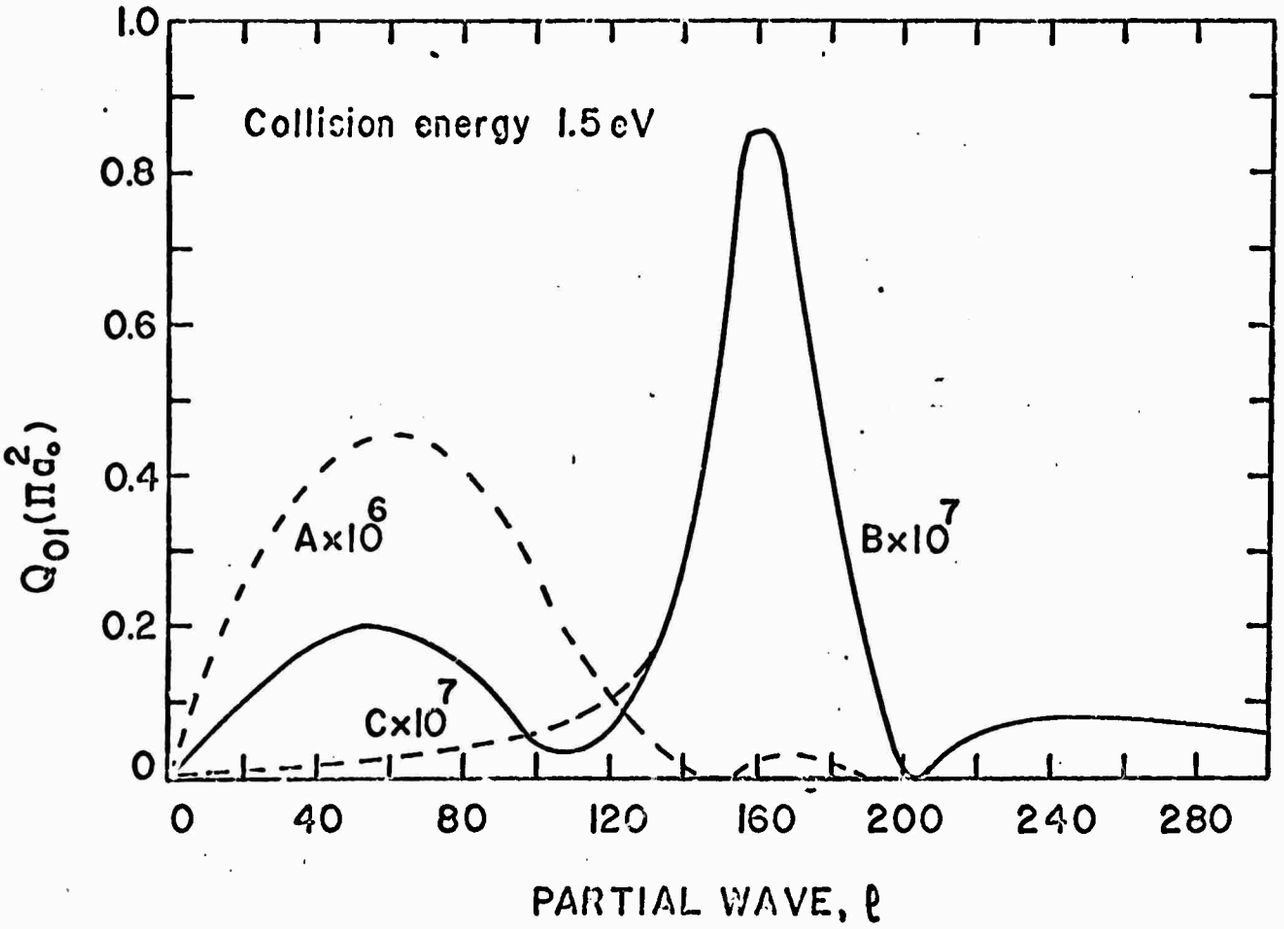

Figure 7. Calculated partial cross sections for the excitation of the first vibrational level of CO by collision with Ar for a soft core potential at a collision energy of 1.5 eV.

A, coupling retained between the first two vibrational levels;

B, coupling retained between the first three vibrational levels;

C, coupling retained between the first four vibrational levels.

Table 5

Total cross sections for the excitation of CO to the first vibrational level by Ar impact

No. of states coupled	2	2	3	4
Potential	LJ	SC	SC	SC
Collision energy* eV	Excitation cross section $Q_{01}(\pi a_o^2)$			
0.266	0.00**	0.00	0.00	0.00
0.600	0.20^{-7}	0.13^{-7}	----	----
1.000	0.35^{-4}	0.21^{-5}	----	----
1.500	0.20^{-2}	0.35^{-4}	0.54^{-5}	0.43^{-5}
2.000	0.14^{-1}	0.25^{-3}	----	----
2.500	0.42^{-1}	0.80^{-3}	----	----

Table 6

Cross sections for the vibrational excitation of CO by He

Potential	LJ	SC	SC	SC
Collision energy* eV	Excitation cross sections (πa_o^2)			
	Q_{01}	Q_{01}	Q_{02}	Q_{12}
0.266	0.0**	0.00	----	----
0.600	1.6^{-2}	1.00^{-3}	0.77^{-9}	6.72^{-6}
1.000	2.4^{-1}	1.28^{-2}	2.60^{-6}	4.40^{-3}
1.500	9.7^{-1}	1.13^{-1}	1.66^{-4}	2.82^{-2}
2.000	1.9	4.06^{-1}	1.89^{-3}	8.68^{-2}
2.500	2.6	8.72^{-1}	8.58^{-3}	1.64^{-1}

* Collision energy relative to the ground state.

** Superscript indicates power of 10 by which number must be multiplied.

8. Discussion

The decrease in the Q_{01} cross section shown in tables 5 and 6 resulting from the use of the soft core potential in place of the Lennard-Jones function leads in turn to correspondingly marked increases in the calculated vibrational relaxation times for CO in the inert gases.

Figure 8 shows the theoretical relaxation time for CO in He obtained by repeating the calculation discussed in section 5 on the basis of the Q_{01}(SC) cross sections given in table 6, in comparison with the experimental results given by Millikan [5].

It can be seen that the agreement with experiment is now much improved. The theoretical results lie within a factor of three of experiment, except at temperatures below 300°K where there is a sharp decrease in the temperature dependence of the calculated relaxation time.

In view of the additional approximations that were required to establish the soft core potential for the CO-He system this result is fully satisfactory and would seem to justify the treatment of CO-inert gas interactions proposed in this report.

However, a similar result is not obtained for the CO-Ar mixture. Figure 9 shows the relaxation times obtained by repeating the calculation discussed in section 5 on the basis of the two state CO-Ar Q_{01}(SC) cross sections given in table 5, in comparison with the experimental result. It can be seen that the theoretical relaxation time is now about a factor of 50 greater than experiment, whereas the previous (LJ) values were about a factor of 4 less.

It is also apparent from table 5 that coupling in additional vibrational states to the calculation does not improve the agreement. Unlike the Lennard-Jones potential, or the CO-He calculation, where coupling in higher states in general leads to an increase in the excitation cross sections, for the soft core potential a decrease is produced at 1.5 eV which yields even smaller vibrational

relaxation times. Figure 7 and table 5 show the result of coupling three or four states. Coupling four states produces a further small reduction in the cross sections, but these results are little different from those for the three state calculation.

This disagreement with experiment is about an order of magnitude worse than the poorest results obtained from the previous applications of the computer code. Evidently the discrepancy is significant and is all the more surprising since the CO-Ar interaction has no peculiar features but should be well represented by the spherically symmetric approximation used here.

As can be seen the cross sections for the excitation of CO by Ar are very small and the possibility that the poor agreement with experiment is a consequence of the numerical rather than the physical treatment of the problem, possibly caused by the weak coupling between the scattering equations, has been investigated. The arbitrary parameters defining such characteristics as the relative scaling between the coupled functions, the position of the starting point for the step integration procedure and step size in the solution of the scattering equations have been varied over wide ranges without altering the results more than a few percent.

The small cross sections are associated with very extensive cancellation occurring throughout the calculation. In fact double precision on the IBM 360 is insufficient for cross sections this small for other than nearest neighbor transitions to be reliably calculated. To determine whether this loss of precision was introducing serious errors into the Q_{01} calculation the code was run in double precision on a CDC 6600 for a collision energy of 1.5 eV. Although the multiple jump cross sections were now accurately obtained it was found that Q_{01} again was virtually unaltered.

Finally, an essentially similar study of N_2-Ar mixtures was carried out by Kindt and Marriott [10], again on the

basis of a potential measured by Jordan et al.[7]. This calculation simply confirmed the CO-Ar results. The N_2 cross sections were somewhat larger and numerically better defined than the corresponding values for CO but the relaxation times were nevertheless within a factor of two of those for CO, as should be the case.

It can only be concluded that the numerical results are quite definite and stable for the form assumed for the soft core scattering potential and that the reason for disagreement with experiment must be looked for elsewhere.

Because of the low efficiency of Ar in vibrationally de-exciting CO the experimental measurements will be very sensitive to trace contamination by molecules such as H_2O or H_2 which are very effective de-exciters of CO. Using the relaxation data for CO in H_2 given by Millikan[5] the degree of contamination that would be required to account for the disagreement between theory and experiment can be estimated. Where f is the fractional contamination by H_2 the relaxation time τ_{mix} for CO in the mixture will be given by the expression

$$\tau_{mix}^{-1} = (1 - f)\tau_{CO-Ar}^{-1} + f\tau_{CO-H_2}^{-1}.$$

At 2000°K, for example, the computed $\tau_{CO-Ar} = 1.2 \times 10^{-2}$ secs
the measured relaxation time in Ar, $\tau_{mix} = 3.5 \times 10^{-4}$ secs
and the measured $\tau_{CO-H_2} = 7 \times 10^{-7}$ secs.

It follows that the degree of contamination by H_2 that would account for the results obtained is $f \approx .002$, or 2000 ppm, which is two orders of magnitude larger than the minimum purity level of "high purity grade Ar" supplied by the Matheson Company. Thus the lack of agreement also cannot be attributed to experimental conditions in any simple way.

At this stage the question remains unresolved. More work needs to be done if cross sections for heavy body collisions are

to be calculated with any confidence for regimes where no experimental work has been performed.

In particular the possibility that collisions involving particles as heavy as Ar are far more sensitive to the form of the scattering potential than is the case for lighter atoms such as He requires investigation.

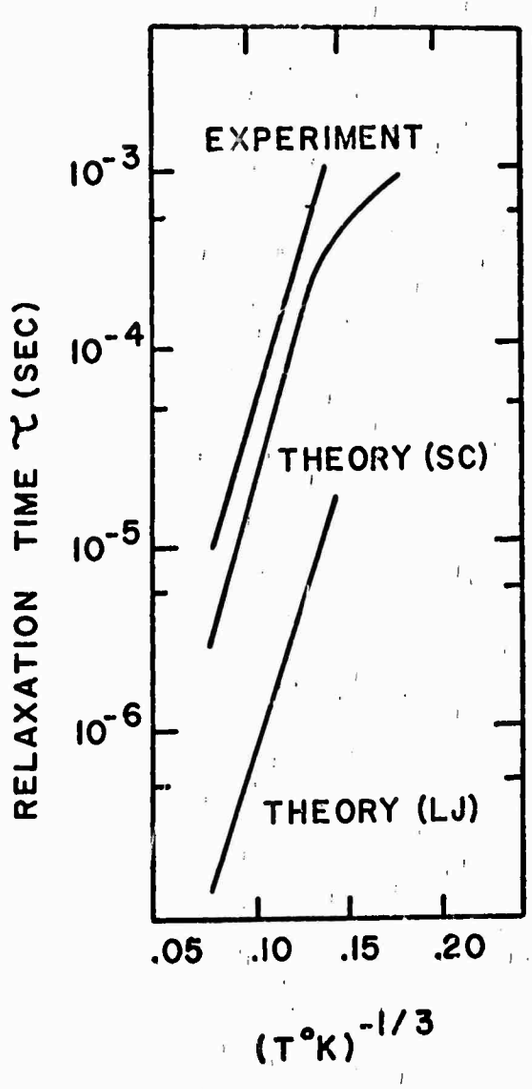

Figure 8. Vibrational relaxation time for CO in He at one atmosphere pressure. Experimental results of Millikan[5]. Theory (LJ); calculated in this paper using a Lennard-Jones potential with coupling between up to the first 4 vibrational states. Theory (SC); calculated in this paper using a soft core potential with coupling between up to 6 vibrational states.

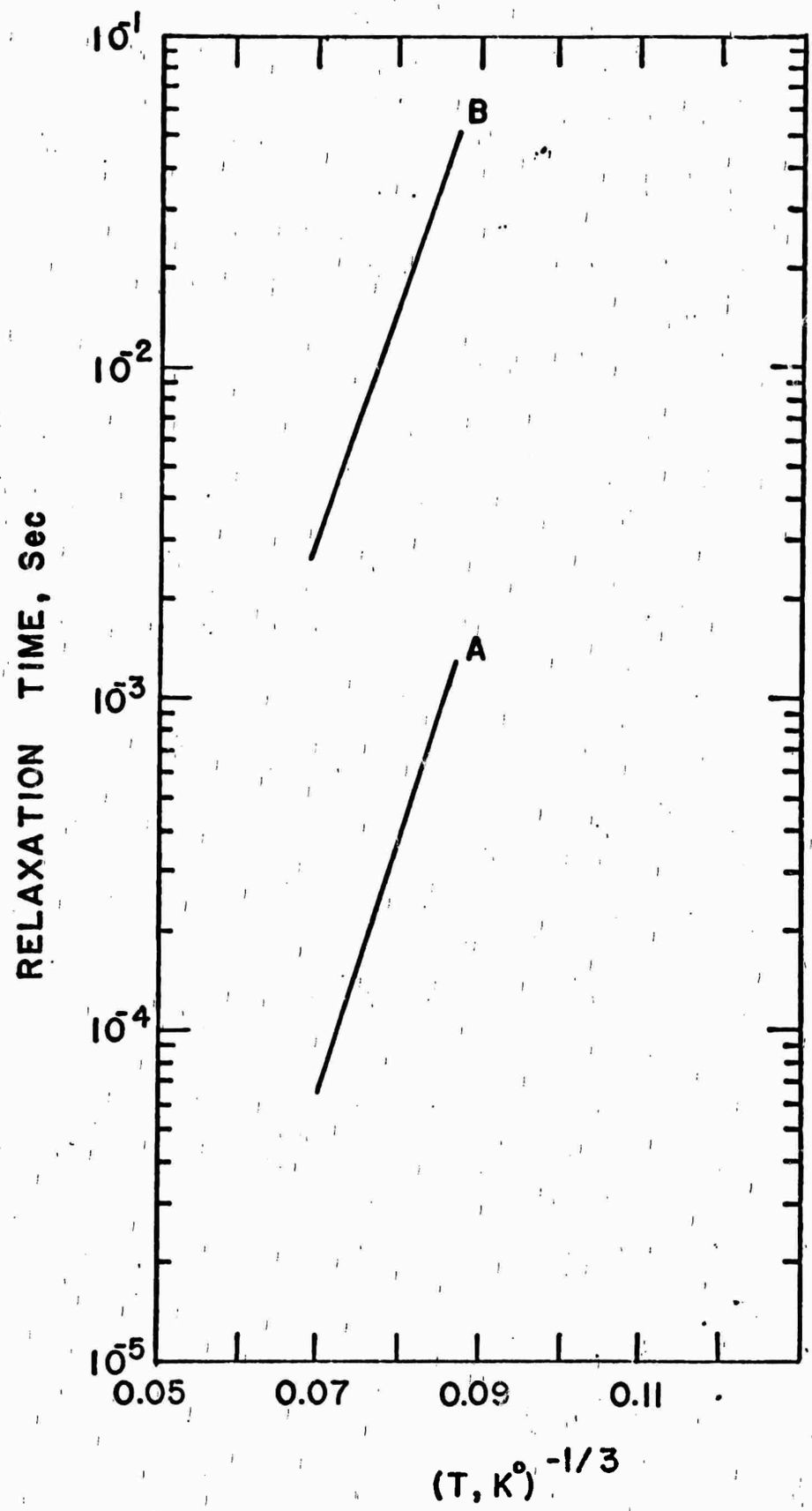

Figure 9. Vibrational relaxation time for CO in Ar at one atmosphere pressure.

A Experimental results of Hooker and Millikan [4].

B Calculated in this Paper using a soft core potential with coupling between the first two vibrational states.

References

1. R. Marriott, Proc. Phys. Soc., 83, 159 (1964).
2. R. Marriott, Proc. Phys. Soc., 84, 877 (1964).
3. F.A. Gianturco and R. Marriott, J. Phys. B, 2, 1332 (1969).
4. W.J. Hooker and R.C. Millikan, J. Chem. Phys., 38, 214 (1963).
5. R.C. Millikan, J. Chem. Phys., 40, 2594 (1964).
6. I. Amdur, E.A. Mason, and J.E. Jordan, J. Chem. Phys., 27, 527 (1957).
7. J.E. Jordan, S.O. Colgate, I. Amdur, and E.A. Mason, J. Chem. Phys., 52, 1143 (1970).
8. J.O. Hirschfelder, F.C. Curtiss, and R.B. Bird, Molecular Theory of Gases and Liquids, (John Wiley, New York (1954)).
9. K.F. Hertzfeld and T.A. Litovitz, Absorption and Dispersion of Ultrasonic Waves, (Academic Press, New York (1959)).
10. G. Kindt and R. Marriott, unpublished report RIES 71-22 (1971).

III. Binary Gas Code and Molecular Laser Modeling

In modeling the transient and steady state operation of molecular laser systems, an understanding of vibrational relaxation processes in addition to the effect of electrons and inert diluents must be obtained. This Section of the report will describe the details of the model code development and its application to gas relaxation systems.

The first part of this Section describes the relaxation of a binary system of diatomic molecules due to both vibration-translation and vibration-vibration processes. As an application of this part of the laser model code, calculations are presented on the system $H_2 + D_2 \rightleftarrows 2HD$. Following this, the electron-vibration rate coefficients are generated together with spontaneous emission coefficients for levels up to v = 29 in CO (both fundamental and overtone). These latter coefficients are needed to compare the laser model calculations directly to side-light measurements on laser systems. Lastly, the transient response of the N_2-CO-He-e system is shown as a preliminary calculation on an actual molecular discharge laser system. In this calculation, 30 levels of both N_2 and CO are included in the code.

III.1 Vibrational Relaxation of a Binary Gas Mixture

It is well known that molecular species are characterized by widely disparate vibrational relaxation times in pure gas systems.[1] The large variation may be illustrated by the diatomic molecules I_2, Cl_2, O_2, and N_2 which have relaxation times at 1000°K of 5×10^{-8}, 5×10^{-7}, 7×10^{-5}, and 10^{-1} atm-sec., respectively.[2] These differences increase at lower temperatures while at high temperatures all gases approach relax with unit collision efficienty.

In treating the vibrational relaxation of gas mixtures in circumstances where the values for the pure gases are widely separated, it is no longer a straight forward problem to correctly designate the relaxation time. The problem is, however, of wide spread applicability since rarely is one interested in knowing the behavior of pure systems (i.e., those systems composed on only one species). This is particularly true of molecular laser systems where many species, both atomic and molecular may be present. The application of vibrational relaxation theories to mixtures is also fundamental to many experimental techniques for determining vibrational temperatures through tracer methods and in determining the effect of impurities on relaxation behavior.

In general, there are two important processes by which vibrational energy is transferred in mixtures. One is the process or processes by which vibrational energy is degraded into other forms of energy such as translation and rotational energies. The second process is vibration-vibration exchange which tends to couple the vibrational energy of the various gases in a mixture. It is the interrelationship of these two processes which determines the relaxation of a gas mixture.

In earlier work,[4] we presented an analysis and discussion on the relative relaxation behavior of harmonic and anharmonic oscillators due to vibration-vibration exchange processes. The results of that study can be summarized for the case of anharmonic oscillators as follows: (1) The steady state vibrational distribution due to vibration exchange processes is non-Boltzmann, in which the upper levels are overpopulated, (2) the time to reach a steady state distribution is an increasing function of vibrational level,[11] (3) total vibrational energy is not conserved on the steady state time scale, and (4) under conditions of high vibrational "temperatures" and low kinetic temperature, population inversion in the upper

vibrational levels is predicted. These conclusions are markedly different from harmonic behavior.[7,8]

III.2 Dynamic Behavior of Gas Mixtures

In this section we extend the previous analysis[4] to the dynamic behavior of relaxing mixtures of diatomic gases, and herein discuss the various relaxation processes involved and their respective relaxation times based on anharmonic models.

For a pure gas it has been previously established[4,9] that a two time scale separation in the relaxation of initially non-equilibrium distributions is a valid assumption for the lower levels of diatomics such as N_2 or CO at low translational temperatures. A short time scale is associated with vibration exchange processes and a longer time scale describes the relaxation to equilibrium through vibration-translation degradation processes. In mixtures of gases we have a similar situation.[4] Rapid vibration exchange processes in each species will redistribute vibrational energy into a steady state distribution which will slowly decay to equilibrium. In addition to these processes, however, the relaxing distributions will be affected by vibrational coupling between the species through vibration exchange reactions.

We have previously shown the strong dependence of vibrational exchange rates on energy defect[10] (i.e., the energy transferred into or out of relative translational energy during an exchange) and consequently, the coupling between two species in a mixture is expected to be strongly dependent on the respective vibrational spacing. For mixtures such as N_2 and CO where the vibrational spacing of the gases is similar (i.e., E_d = 188 cm^{-1} for the $v_{01} - v_{01}$ levels and E_d= 14 cm^{-1} for the $v_{67} - v_{01}$ levels of N_2 and CO, respectively), the exchange rates within each species will not display an energy defect

while rates between species will be characterized by a rather large defect (i.e., 100 cm^{-1}), thus, in the harmonic model, a slight time separation in the pure gas vibrational exchange processes and the coupling between species is expected.

For a mixture of gases such as N_2 and NO, the energy defect between species is considerably larger than that exhibited in either of the pure gases and consequently, three distinct time scales should be evident. The first time scale will feature rapid vibrational rearrangement in each molecule leading to a steady state distribution as previously[4] predicted. A second and longer time scale will describe the coupling of the two vibrational distributions to form a second steady state distribution which will then proceed toward equilibrium through vibration-translation processes on a third time scale.

As the energy defect between two species in a mixture is increased by suitably changing one of the species, eventually a merging of the time scales for mixture coupling and vibration-translation processes for one of the species will occur. This situation is evident for N_2 and O_2 mixtures at low temperatures (i.e., < 3000°K) as demonstrated by the measurements of Millikan and White.[3]

In order to illustrate these various time scales for the case of mixture relaxation, the master equation for the time evolution of a binary mixture has been formulated and numerically integrated.

The Master Equation

The master equation for a binary mixture may be written:[4,7]

$$\frac{dn_r}{dt} = \sum_s (P_{sr} n_s n - P_{rs} n_r n) + \sum_s \left[\sum_{l \neq m} \sum_m (P_{sr}^{lm} n_s n_l - P_{rs}^{ml} n_r n_m) \right]$$
$$+ \sum_s (Q_{sr} n_s N - Q_{rs} n_r N) + \sum_s \left[\sum_{S \neq R} \sum_R (Q_{sr}^{SR} n_s N_S - Q_{rs}^{RS} n_r N_R) \right] \qquad (1)$$

in which n_i is the population of the i-th vibrational level; n is the total number density of species A; N_i and N, the corresponding densities of species B; P_{sr} is the rate constant for the process:

$$n_s + n \longrightarrow n_r + n \qquad (2)$$

in which vibrational energy corresponding to $E_r - E_s$, the difference between the energies of the r-th and s-th states in species A, is transferred to or from translational energy; P_{sr}^{lm} is the rate constant for the process:

$$n_s + n_l \longrightarrow n_r + n_m \quad , \qquad (3)$$

in which vibrational energy is exchanged within species A, the slight energy defect being compensated by translational energy; and Q_{sr} and Q_{sr}^{SR} are the analogous rate constants for the vibration-translation and vibration-vibration energy transfer processes involving the cross terms between species A and B:

$$n_s + N \longrightarrow n_r + N \quad , \qquad (4)$$

and

$$n_s + N_S \longrightarrow n_r + N_R \ . \qquad (5)$$

In our earlier work,[4] we concluded that in the pure gas case, only single quantum processes need be considered. However, for mixtures of gases with greatly differing vibrational spacing there is a possibility that resonant vibration-vibration exchange might involve a double quantum transition in one of the species. In general, for the lower vibrational levels, these processes will be slow in comparison to single quantum processes due to the form of the rate expressions[10] and we will restrict ourselves in this report to systems wherein only single quantum processes are important. Evidently this is not a major limitation since most of the diatomic systems of interest fall within this classification.

This restriction, coupled with the use of the detailed balance conditions,

$$\begin{aligned} P_{r,r+1} &= P_{r+1,r}\, e^{-(E_{r+1} - E_r)/kT}, \\ Q_{r,r+1} &= Q_{r+1,r}\, e^{-(E_{r+1} - E_r)/kT}, \\ P^{ml}_{rs} &= P^{lm}_{sr}\, e^{-(E_s + E_l - E_r - E_m)/kT}, \end{aligned} \qquad (6)$$

and

$$Q^{RS}_{rs} = Q^{SR}_{sr}\, e^{-(E_s + F_S - E_r - F_R)/kT},$$

where F_I represents the vibrationel energy of the I-th level of species B above the zeroth level, permits the master equation to be written as:

$$\frac{dn_r}{dt} = P_{r+1,r}\left[n_{r+1}\, n - e^{-(E_{r+1}-E_r)/kT}\, n_r n \right] - P_{r,r-1}\left[n_r n - e^{-(E_r-E_{r-1})/kT}\, n_{r-1}\, n \right]$$

$$+\sum_s P^{s-1,s}_{r+1,r}\left[n_{r+1}\, n_{s-1} - e^{-(E_{r+1}+E_{s-1}-E_r-E_s)/kT}\, n_r\, n_s \right]$$

$$-\sum_s P^{s,s+1}_{r,r-1}\left[n_r\, n_s - e^{-(E_r+E_s-E_{s+1}-E_{r-1})/kT}\, n_{s+1}\, n_{r-1} \right]$$

$$+Q_{r+1,r}\left[n_{r+1}\, N - e^{-(E_{r+1}-E_r)/kT}\, n_r N \right] - Q_{r,r-1}\left[n_r N - e^{-(F_r-E_{r-1})/kT}\, n_{r-1} N \right]$$

$$+\sum_R Q^{R-1,R}_{r+1,r}\left[n_{r+1}\, N_{R-1} - e^{-(E_{r+1}+F_{R-1}-E_r-F_R)/kT}\, n_r\, N_R \right]$$

$$-\sum_R Q^{R,R+1}_{r,r-1}\left[n_r\, N_R - e^{-(E_r+F_R-F_{R+1}-E_{r-1})/kT}\, n_{r-1}\, N_{R+1} \right] + \phi_r , \qquad (7)$$

where ϕ_r is a production or destruction source of n_r. In later sections of this report, this term will include the excitation of vibrational levels by hot electrons and the spontaneous emission associated with infrared active molecules, e.g. CO.

Equation (7) formally describes the rate of change of n_r with time in the absence of dissociation. The effect of dissociation on vibrational distributions is currently under study. Three distinct types of terms are present. The most familiar are those for the transfer of vibrational to translational energy and the reverse (i.e., $P_{s,s-1} n_s n$). These processes will be designated as VT. The vibration-vibration exchange terms in a single species (i.e., $P^{s-1,s}_{r+1,r}\, n_{r+1}\, n_{s-1}$) will be designated by VV_{A-A} or VV_{B-B}, while the exchange terms between species

(i.e., $Q^{R-1,R}_{r+1,r}\, n_{r+1}\, N_{R-1}$) will be noted as VV_{A-B}.

The set of equations (7) with the rate constants outlined in the next Section have been numerically integrated by the Runge-Kutta-Merson technique.[14] This numerical technique has been used extensively for the integration of large sets of coupled non-linear ordinary differential equations such as are found in modelling coupled chemical reactions. A particular feature of the code as taken from the work of Keneshea[14] is the use of a version of the steady state (S-S) approximation for those equations which satisfy an appropriate criterion. In a coupled set of rate equations such as occur for vibrational relaxation, the equation can be written

$$\frac{dn_r}{dt} = \sum F_r - \sum R_r \cdot n_r \qquad (8)$$

where the $\sum F_r$ and $\sum R_r$ terms may be complicated functions of all the other concentrations and rate coefficients. Under conditions where the magnitudes of both $\sum F_r$ and the term $\sum R_r \cdot n_r$ are large but their difference very small, the time progress in the normal Runge-Kutta integration is very slow, i.e. the set of equations become "stiff." In the Keneshea version of the code as used here, each equation is checked to determine if it satisfies the S-S criterion, meaning the magnitude of the $\sum F_r$ term is large but the derivative is small. When this criterion is passed the equation is iterated over the Δt time step using an algebraic algorithm as shown below.

For conditions under which $\sum F_r$ and $\sum R_r$ are both large, rather than use the canonical S-S assumption

$$\frac{dn_r}{dt} = 0 \qquad (9)$$

which leads to

$$n_r = \frac{\sum F_r}{\sum R_r} \quad , \tag{10}$$

the more realistic assumption is made that the $\sum F_r$ and $\sum R_r$ terms are effectively constant over the Δt step leading to a first order ordinary differential equation. The solution is

$$n_r(t + \Delta t) = \left(n_r(t) - \frac{\sum F_r}{\sum R_r} \right) e^{-\sum R \cdot \Delta t} + \frac{\sum F_r}{\sum R_r} \quad . \tag{11}$$

This solution is used for all equations satisfying the steady state criterion and is iterated over a Δt step together with the other equations which continue to be integrated by the Runge-Kutta-Merson technique. When an equation ceases to satisfy S-S, it is automatically returned to the R-K-M subroutine for integration.

By the use of this S-S algorithm, the time step in the integration can be kept large while not sacrificing either stability or accuracy in the coupled set of equations.

The vibration-vibration rate coefficients used in the code are adapted from a model presented by Rapp and Englander-Golden[12]. The derivation of the rate coefficient is given in Appendix I while the actual expression used is

$$P_{sm}^{rn} = 1.508^{-12} \mu^{7/6} L^{10/3} \sigma^2 E_d^{4/3} T^{5/6} U_{rn}^2 U_{sm}^2 \cdot \left| \exp -1.32 (L E_d)^{2/3} \frac{\mu}{T}^{1/3} \right| \tag{12}$$

where

μ = reduced mass in molar units

L = exponential potential parameter ($\mathring{A}$)

σ = hard sphere diameter ($\mathring{A}$)

T = kinetic temperature (°K)

E_d = energy defect between vibrational quanta being exchanged (cm^{-1})

and

U_{rn} = matrix element for the r → n vibrational transition

The matrix elements used are modified Harmonic Oscillator matrix elements[13] in which the actual energy spacing between vibrational units is used instead of the constant spacing assumed in the H-D model. Very close agreement has been found for these matrix elements by comparison to Morse oscillator results as shown in Table I.

Vibration-translation rate coefficients have been taken from measured relaxation times using a harmonic oscillator model[1]. The expression used is

$$P_{rn} = \frac{RT}{p\tau}\left(1 - e^{-hcw/kT}\right)^{-1}\left(\frac{U_{rn}^2}{U_{01}^2}\right) \qquad (13)$$

where $p\tau$ is the measured relaxation time. Scaling with vibrational level is given by the square of the vibrational matrix elements.

III.3 Application of the Binary Code to the $H_2 + D_2$ Reaction

As a test for the model code and to interpret the results of recent experiments on the reaction

$$H_2 + D_2 \rightleftarrows 2HD \qquad (14)$$

the vibrational relaxation code has been applied to this system. Previous studies[15] have noted the following facts regarding this reaction[16]:

(a) in the phenomenological rate expression, the exponent of the concentrations of H_2 and D_2 are not the same,

(b) the rate appears quadratic in time,

(c) vibrational energy in either H_2 or D_2 appears necessary to initiate the reaction.

Table I

BOUND-BOUND MATRIX ELEMENTS

FOR N_2

Element	Harmonic	Morse
0-1	.08058	.08062
1-2	.11505	.11366
2-3	.14227	.13876
3-4	.16589	.15973
4-5	.18729	.17800
5-6	.20721	.19441
6-7	.22607	.20927
7-8	.24413	.22305
8-9	.26160	.23580
9-10	.27862	.24771
10-11	.29529	.25900
11-12	.31169	.26959
12-13	.32790	.27970
13-14	.34397	.28927
14-15	.35996	.29854
15-16	.37589	.30716
16-17	.39182	.31575
17-18	.40777	.32363
18-19	.42376	.33154
19-20	.43984	.33889
20-21	.45603	.34597
21-22	.47234	.35298
22-23	.48881	.35964
23-24	.50545	.36623
24-25	.52229	.37228
25-26	.53935	.37855
26-27	.55665	.38445
27-28	.57422	.39014
28-29	.59208	.39541
29-30	.61023	.40099
30-31	.62872	.40592
31-32	.64756	.41108
32-33	.66680	.41618
33-34	.68642	.42109

Theoretical studies have not been successful in understanding the small activation energy, i.e. 42 kcal/mole, which is considerably less than the dissociation energy of either H_2 or D_2,[17] although studies of this 4 center system cannot be fully treated.

The particular experiments modeled by detailed calculations involve the Raman excitation of the $v = 1$ level of H_2 in the presence of D_2 and the subsequent formation of HD. The reaction vessel initially has 5 atm each of H_2 and D_2 at room temperature and the raman excitation is postulated to give roughly 1% $H_2(v = 1)$ per pulse. Following many pulses, the reaction mixture is analyzed for HD. The experiments suggest approximately $5 \times 10^{+16}$ HD molecules/cc produced per pulse.

In performing this model calculation, in addition to the VV and VT processes which are operative in and between H_2 and D_2, the following reaction terms were included in the code:

$$H_2(v) + D_2 \rightleftarrows 2HD \qquad k(v) = \begin{cases} 10^{-12} & \text{for } v \geq 3 \\ 0 & \text{for } v < 3 \end{cases} \tag{15}$$

$$D_2(v) + H_2 \rightleftarrows 2HD \qquad k(v) = \begin{cases} 10^{-12} & \text{for } v \geq 4 \\ 0 & \text{for } v < 4 \end{cases} \tag{16}$$

The rate coefficients are assumed to be zero until a vibrational level is reached approximately consistent with the measured activation energy. The VT rate coefficients used, i.e. the relaxation times, are taken from Kiefer and Lutz[18] while the VV rate coefficients are calculated from the model in the previous section.

In Figure 1 is shown the transient behavior of representative vibrational levels and in Figure 2, the HD produced via the preceeding reactions for the case in which 1% $H_2(v = 1)$ is

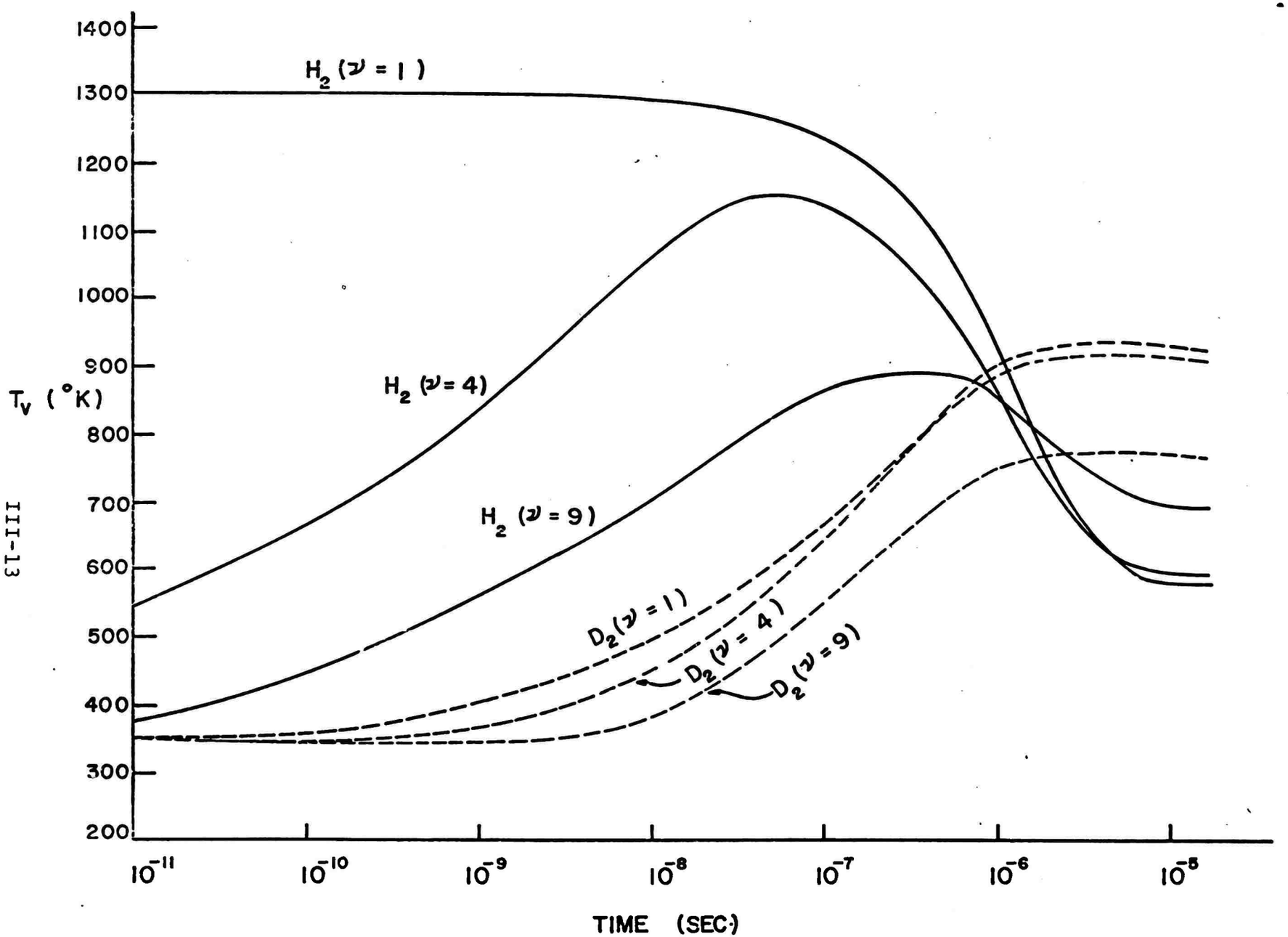

Figure 1A: Relaxation of Vibrational Energy in H_2- D_2 Mixtures.

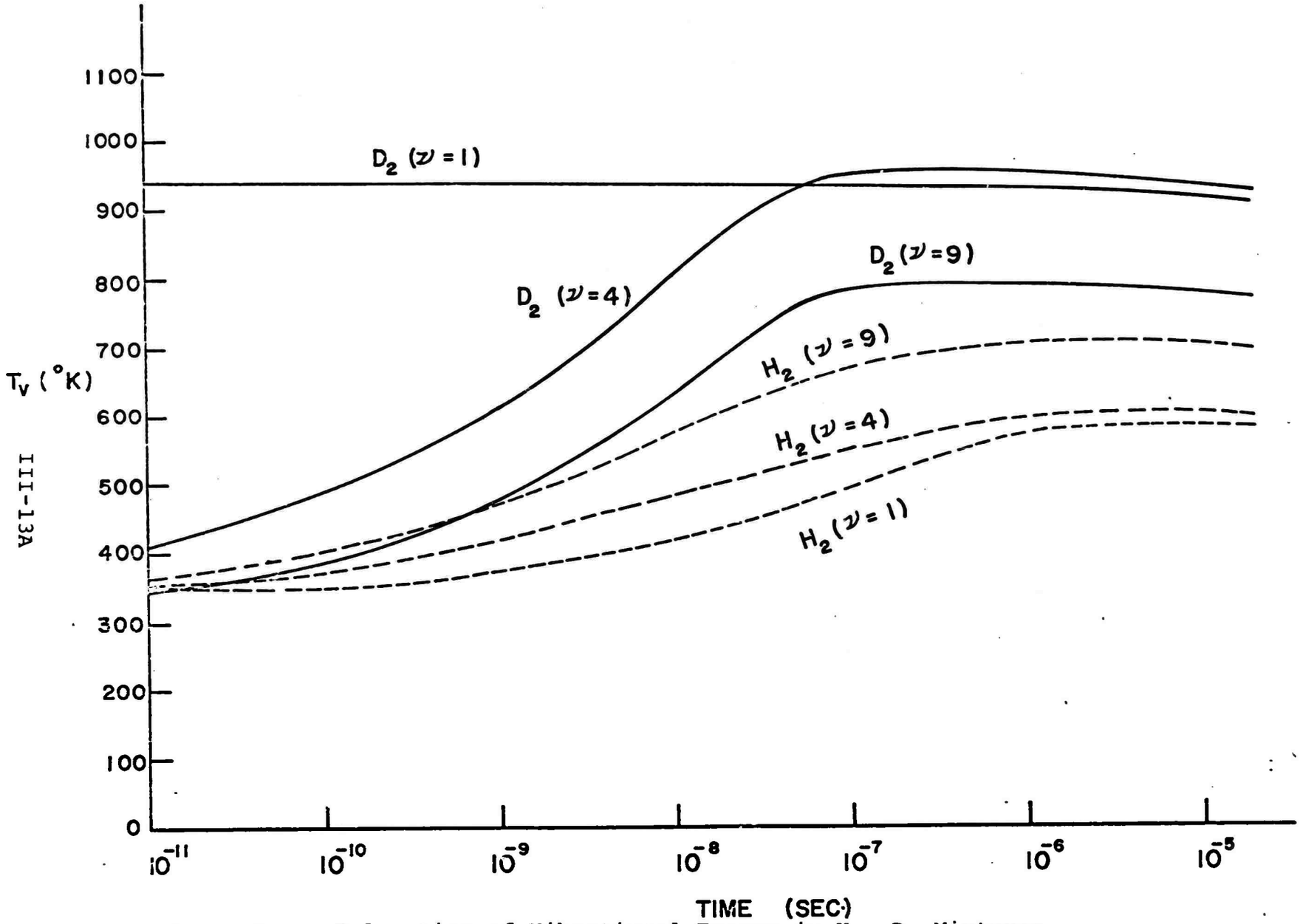

Figure 1B: Relaxation of Vibrational Energy in H_2- D_2 Mixtures.

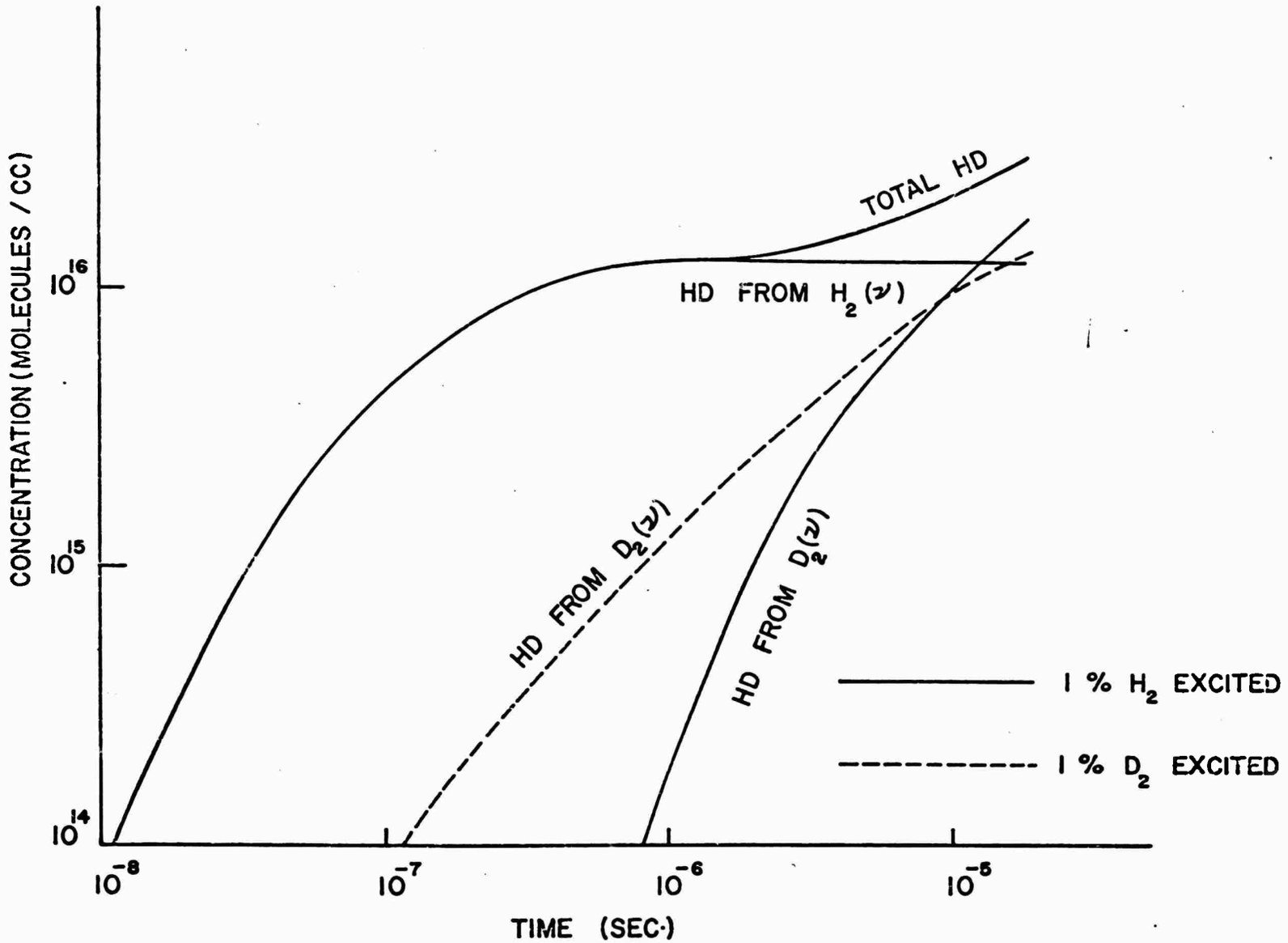

Figure 2 - HD Production in $H_2 + D_2 \rightleftarrows 2HD$

excited. The results show production rates of HD consistent with experimental observation but the most important point is that even though H_2 vibrational levels where initially excited, the majority of the HD formed is through vibrationally excited D_2. This is a direct result of the VV processes which tend to preferentially pump D_2 levels from H_2 due to the smaller vibrational spacing. The time scales for this exchange are displayed in Figure 1. It is important to note that if the initial conditions are 1% $D_2(v = 1)$, then the HD produced is again of the order of $5 \times 10^{+16}$ molecules/cc, but for this case there is essentially no contribution due to the vibrationally excited H_2 reaction, as expected from the larger vibrational spacing. The details of this calculation are currently being prepared.[19]

III.4 Excitation of N_2 and CO Vibrational Levels by Electrons

The excitation of vibrational levels of N_2 and CO by electrons is an important process in molecular discharges, molecular lasers and in the upper atmosphere. In studying the transient and steady state behavior of molecular systems in which hot electrons are present, the rate coefficients characterizing the coupling between the electrons and vibrational levels are required. In this section, rate coefficients are calculated from cross section data of Schulz[20] and Chen[21]. Of particular interest is the temperature dependence of the rate coefficients at elevated temperatures (appropriate to molecular laser systems) and the scaling of the rate coefficients with increasing vibrational level.

Analytical Development

The rate coefficient, k(T) can be defined in terms of the cross section, Q(v), as

$$k(T) = \int_{-\infty}^{\infty} Q(v)\ v\ f(\vec{v})\ d\vec{v} \qquad (17)$$

where $f(\vec{v})$ is the Maxwell-Boltzman distribution of velocities. By transforming $f(\vec{v})\,d\vec{v}$ to a distribution of speeds, equation (17) can be written

$$k(T) = 4\pi \left(\frac{m}{2\pi kT}\right)^{3/2} \int_{0}^{\infty} Q(v) v^3 \exp\left\{\frac{-mv^2}{2kT}\right\} dv. \qquad (18)$$

Equation (18) can be easily changed to the energy representation, yielding the following rate coefficient:

$$k(T) = 8\pi \left(\frac{1}{2\pi kT}\right)^{3/2} \left(\frac{1}{m}\right)^{1/2} \int_{0}^{\infty} Q(E)\ E \exp\left\{-E/kT\right\} dE \qquad (19)$$

where $E = \frac{1}{2} m v^2$, m being the reduced mass of the collision (essentially the electron mass).

The available data on electron excitation cross sections for N_2 and CO[20] can be fit over a limited electron energy range $E_1 \rightarrow E_2$, where $E_2 > E_1$ by

$$Q(E) = AE + B \qquad (20)$$

where A and B are constants determined by the end point values E_1, Q_1 and E_2, Q_2. Thus

$$A = \frac{Q_2 - Q_1}{E_2 - E_1}$$

$$B = \frac{E_2 Q_1 - E_1 Q_2}{E_2 - E_1} . \qquad (21)$$

Over the energy range $E_1 \rightarrow E_2 = \Delta E_{12}$, the integral in (19) can be integrated, yielding

$$k(T)\Big|_{E_2}^{E_1} = 8\pi(2\pi kT)^{-3/2}(m)^{-1/2}\left[e^{-E/kT}(kT)\left\{(2kTA+B)(E+kT)+AE^2\right\}\Big|_{E_2}^{E_1}\right] \qquad (22)$$

and

$$k(T) = \sum_{\Delta E_{12}} k(T)\Big|_{E_2}^{E_1} \qquad (23)$$

Equations (22) and (23) have been programmed to yield excitation rate coefficients as a function of the electron temperature using input cross section data.

Results and Discussion

The rate coefficients for the excitation of vibrational levels of N_2 and CO by electrons in the electron temperature range 1000°K to 30,000°K using the measured cross section data of Schulz[20] are shown in Figures 3 and 4, respectively. The complete numerical results for these cases are available elsewhere[22], together with the cross section data used in the calculation. In general, the error limits on the calcu-

Figure 3

VIBRATIONAL EXCITATION RATE COEFFICIENTS FOR N_2 (v→v') BY ELECTRONS

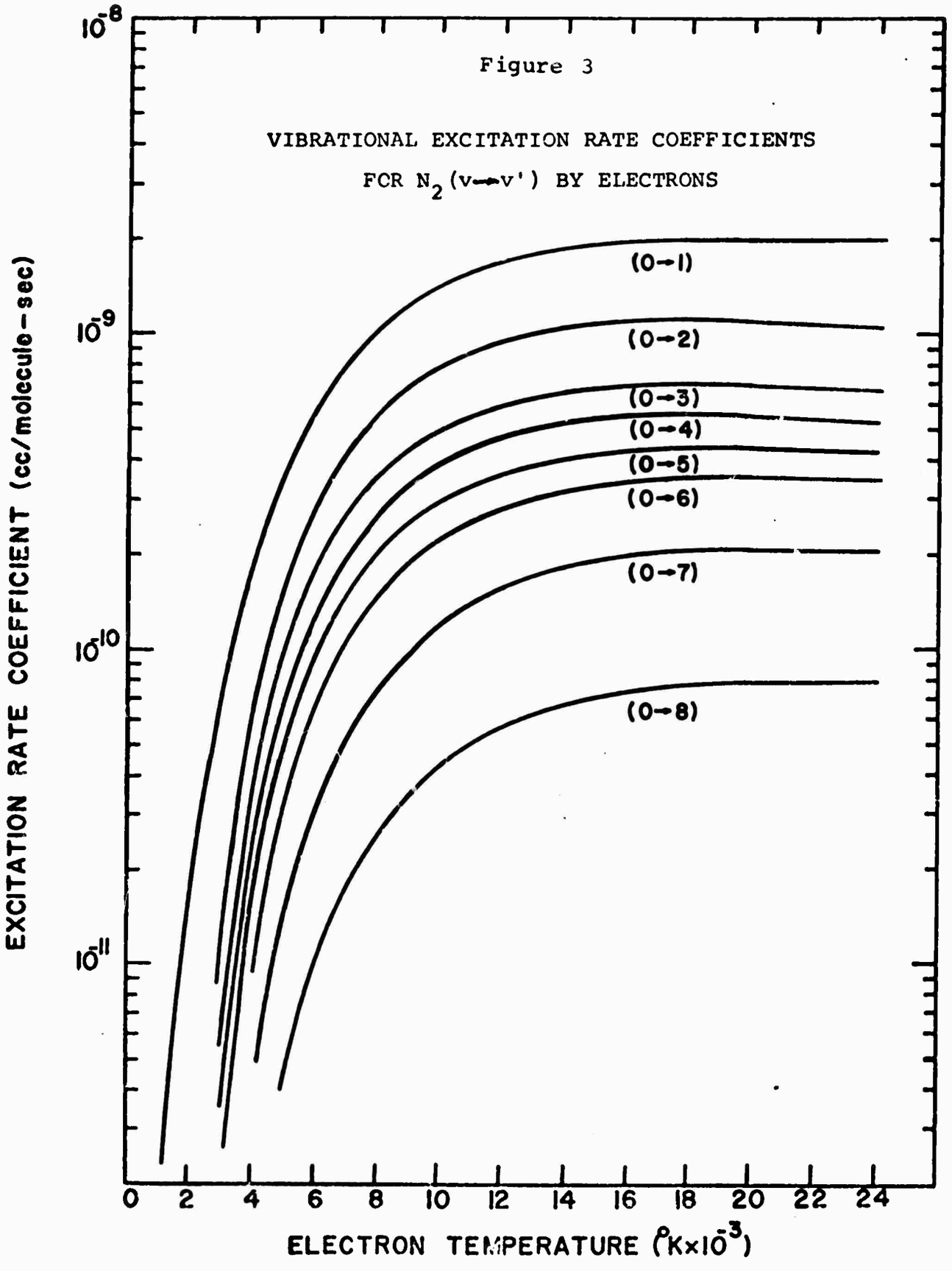

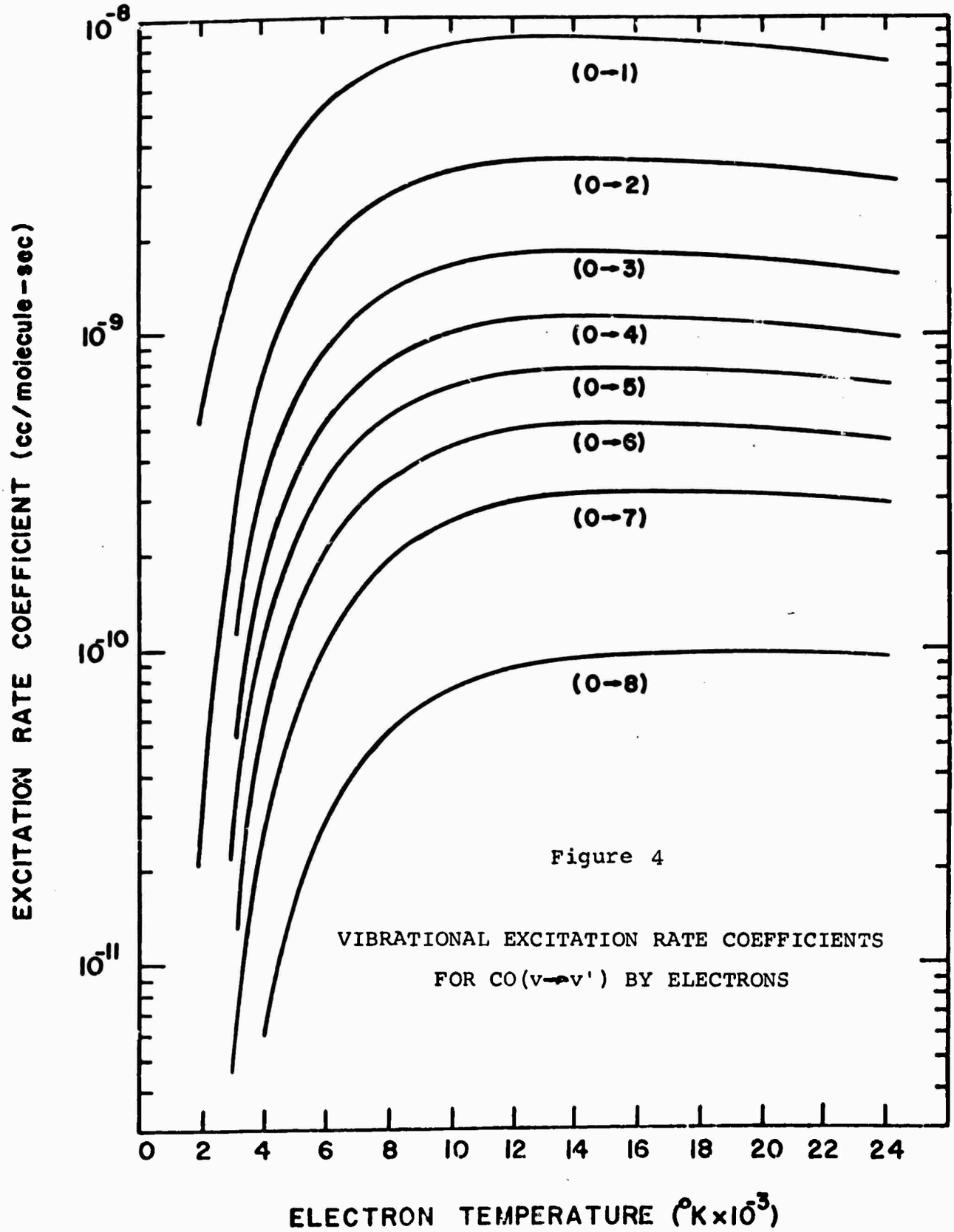

Figure 4

VIBRATIONAL EXCITATION RATE COEFFICIENTS FOR CO(v→v') BY ELECTRONS

lated rate coefficients are about ± 20%.

The spacing of the electron excitation rate coefficients for progressively larger quantum changes reflects the negative ion mechanism responsible for the excitation process. In both N_2 and CO, the negative ions are unstable by 1.89 ev[21,23] and 1.3 ev[21], respectively, corresponding to about the 6th vibrational level of each molecule. The spacing of the rate coefficients indicates a rather close coupling between levels near $v = 6$ while quantum changes greater than 6 show a considerably reduced coupling, i.e. a wider spacing.

The excitation rate coefficients calculated from the theoretical cross sections of Chen[2] are tabulated together with the corresponding cross sections elsewhere[22]. The general agreement between the calculated and measured values is within the accuracy of the overall rate coefficients, i.e. 20%.

By observing the calculated rate coefficients derived from Chen's cross sections, some indication of the scaling necessary with increasing vibrational level can be obtained. Figures 5 and 6 show this relationship for $\Delta v = 1$ and $\Delta v = 5$ processes, respectively. No trend in the calculated values are noted with increasing vibrational level in the electron temperature range between 10,000°K and 30,000°K, therefore, to within the accuracy of these calculations all excitation processes with the same Δv change can be assigned the same value as the $v = 0$ excitation case at any given electron temperature.

It is also very important to note that above about 10,000°K the electron excitation rate coefficients are effectively independent of temperature. This fact means that in calculating the vibrational distributions in a discharge environment in which the electron temperature is greater than

Figure 5

VIBRATIONAL EXCITATION RATE COEFFICIENTS

FOR N_2 (v→v') BY ELECTRONS

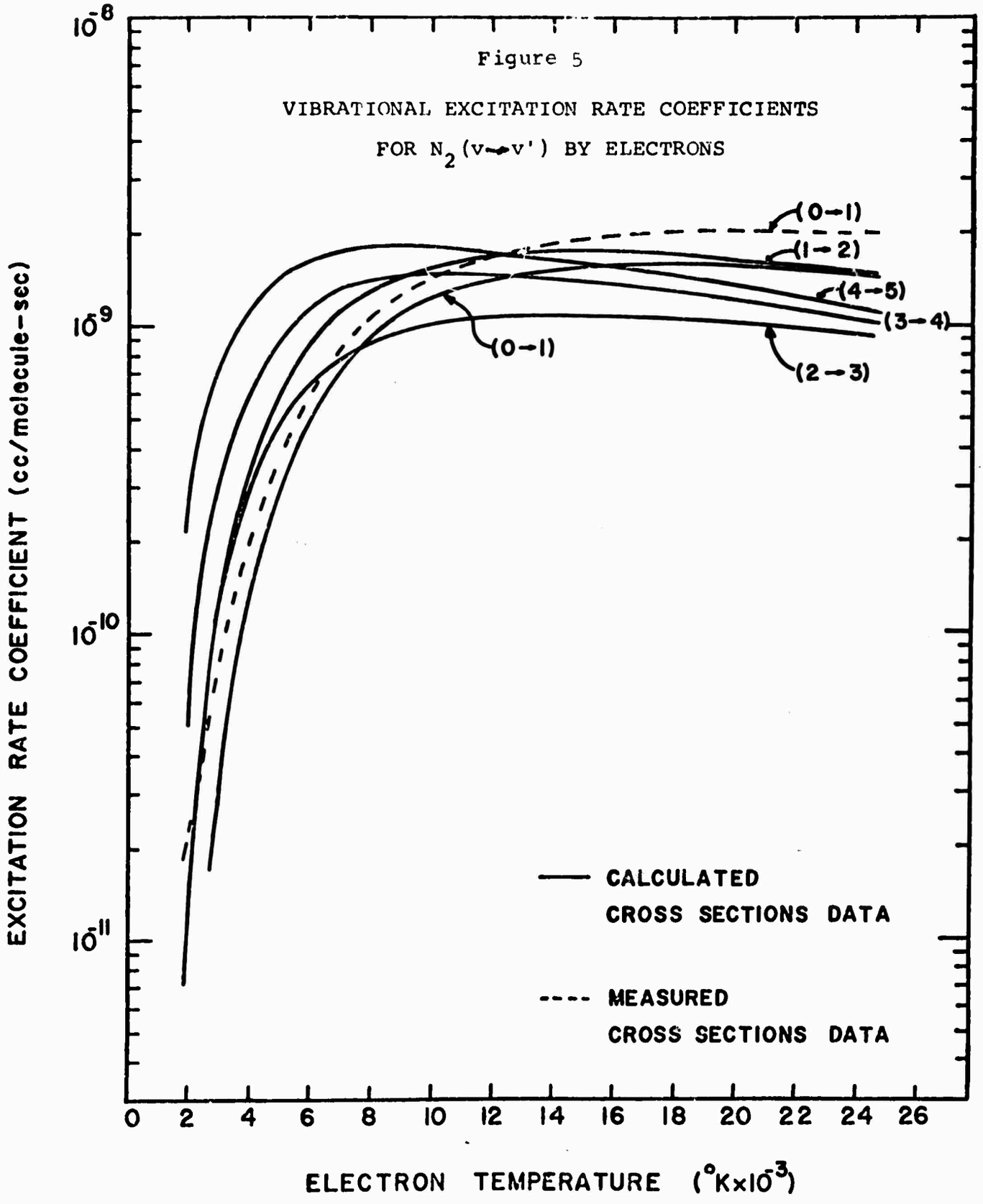

Figure 6

VIBRATIONAL EXCITATION RATE COEFFICIENTS FOR N_2 (v→v') BY ELECTRONS

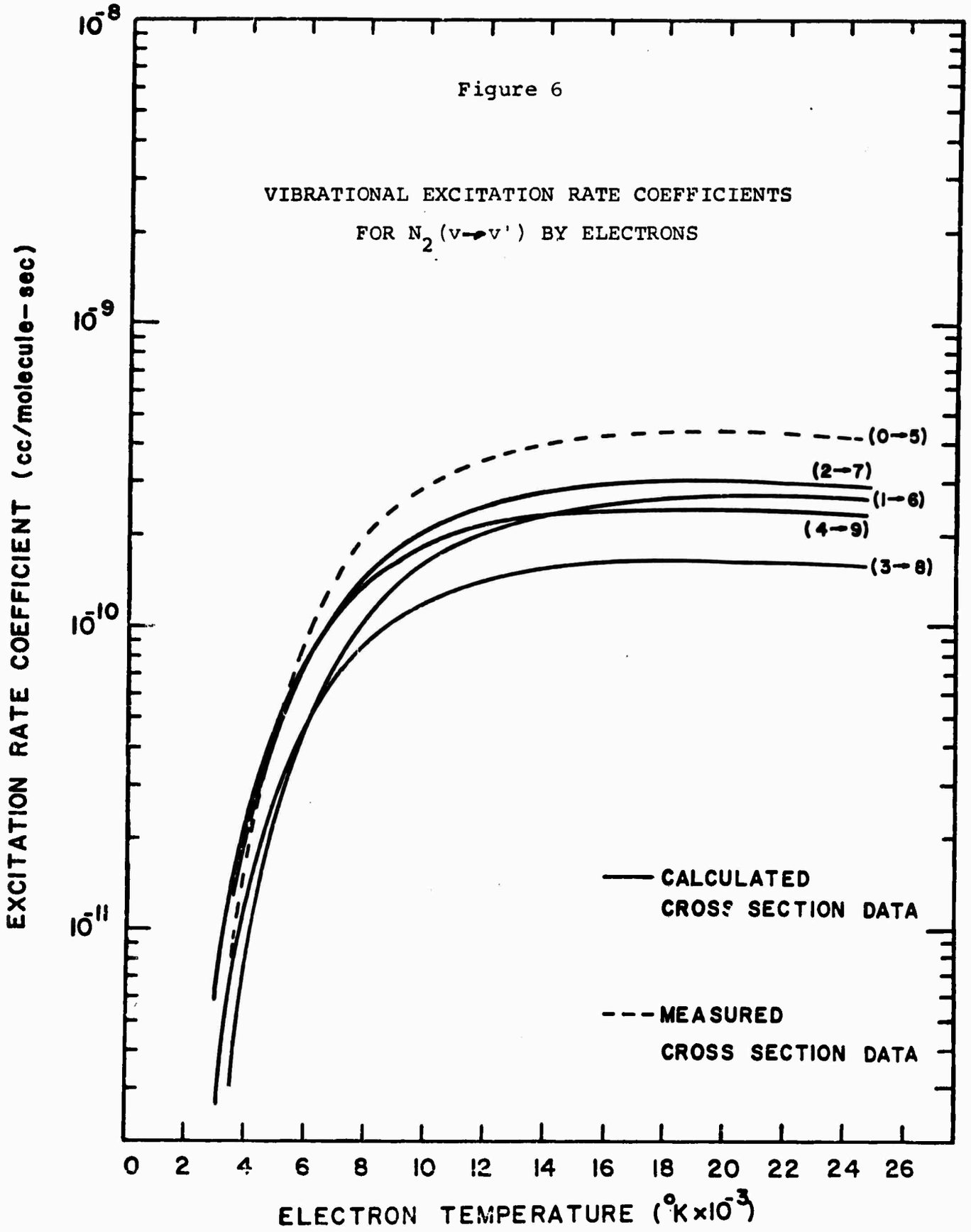

this value, no account has to be taken of the non-Boltzmann electron distributions calculated to be present[25]. This is not the case for excitation of electronic states since these processes will be very sensitive to the high energy electron tail.

III.5 Spontaneous Emission Coefficients for CO

As part of the modeling of molecular lasers, the spontaneous emission emitting from vibrational transitions in the infrared must be characterized. This serves two purposes; firstly, the emission from higher lying vibrational levels can be a significant energy loss mechanism in distorting the vibrational distribution and secondly, in evaluating the model laser code through side-light emission the code must be able to generate artificial spectra. In this section, we present the fundamental and first overtone Einstein Coefficients for Spontaneous Emission calculated from the data of Young and Eachus[24].

Young and Eachus have evaluated 4 cubic dipole moment functions and have concluded that

$$M(r) = \pm 0.112 + 3.11(r - r_e) - 0.15(r - r_e)^2 - 2.36(r - r_e)^3 \quad (24)$$

is best, based on the relative rotational line intensities in the overtone bands of CO. Using the integrated band intensities for the fundamental and overtone bands of

$$\alpha_{fundamental} = 261 \text{ amagat}^{-1}\text{cm}^{-2}$$

and

$$\alpha_{overtone} = 1.88 \text{ amagat}^{-1}\text{cm}^{-2}$$

the following table of Einstein Coefficients has been generated and incorporated into the laser model code. Current work is concentrated on a subroutine to generate the entire artificial spectrum in the vibration-rotation bands including an appropriate slit function.

III.6 Preliminary Laser Model Calculations

The several sections of the numerical code as described in the previous pages has been incorporated into a preliminary laser code. Currently the code is capable of handling up to 40 levels in each of two diatomic molecules, i.e. N_2 and CO, while also including excitation via hot electrons and VT processes due to an inert diluent. The code is particularly suited to study the transient response of the vibrational distributions of both diatomics to a steady state electron temperature such as would occur in a direct discharge laser. Preliminary calculations have been performed to check out the operation of the code.

Figure 7 shows the time development in the vibrational distribution of CO in the presence of 20,000°K electrons using a 20 level model for CO in the presence of He. The structured appearance to the early time profile is due to the non-uniform electron-vibrational coupling rates as shown in Figures 3 and 4. As time progresses, VV processes become important and smooth out the vibrational profile. Further, due to the decreasing vibrational spacing with increasing quantum number, higher lying vibrational levels are pumped preferentially at the expense of lower ones as has been pointed out before[4,7,9]. At long times, when the lower vibrational levels have reached a steady state value, the upper levels continue to grow and, in fact, show population inversion. This behavior of the 20 level code has been traced to the termination of the set of vibrational equa-

Table II

Relative Einstein Coefficients for Spontaneous Emission for CO

upper vibrational level	fundamental	overtone
1	1.00	----
2	1.93	1.00
3	2.78	3.00
4	3.53	5.96
5	4.21	9.89
6	4.81	14.74
7	5.35	20.48
8	5.74	27.03
9	6.23	34.36
10	6.58	42.43
11	6.88	51.17
12	7.14	60.54
13	7.35	70.79
14	7.60	81.62
15	7.73	92.99
16	7.83	104.82
17	7.90	117.05
18	7.93	131.84
19	7.94	147.24
20	7.83	160.27
21	7.69	173.80
22	7.53	187.53
23	7.35	201.19
24	7.16	214.94
25	7.00	228.60
26	6.74	242.13
27	6.51	255.45
28	6.27	268.52
29	5.82	281.40

CO LASER TIME HISTORY

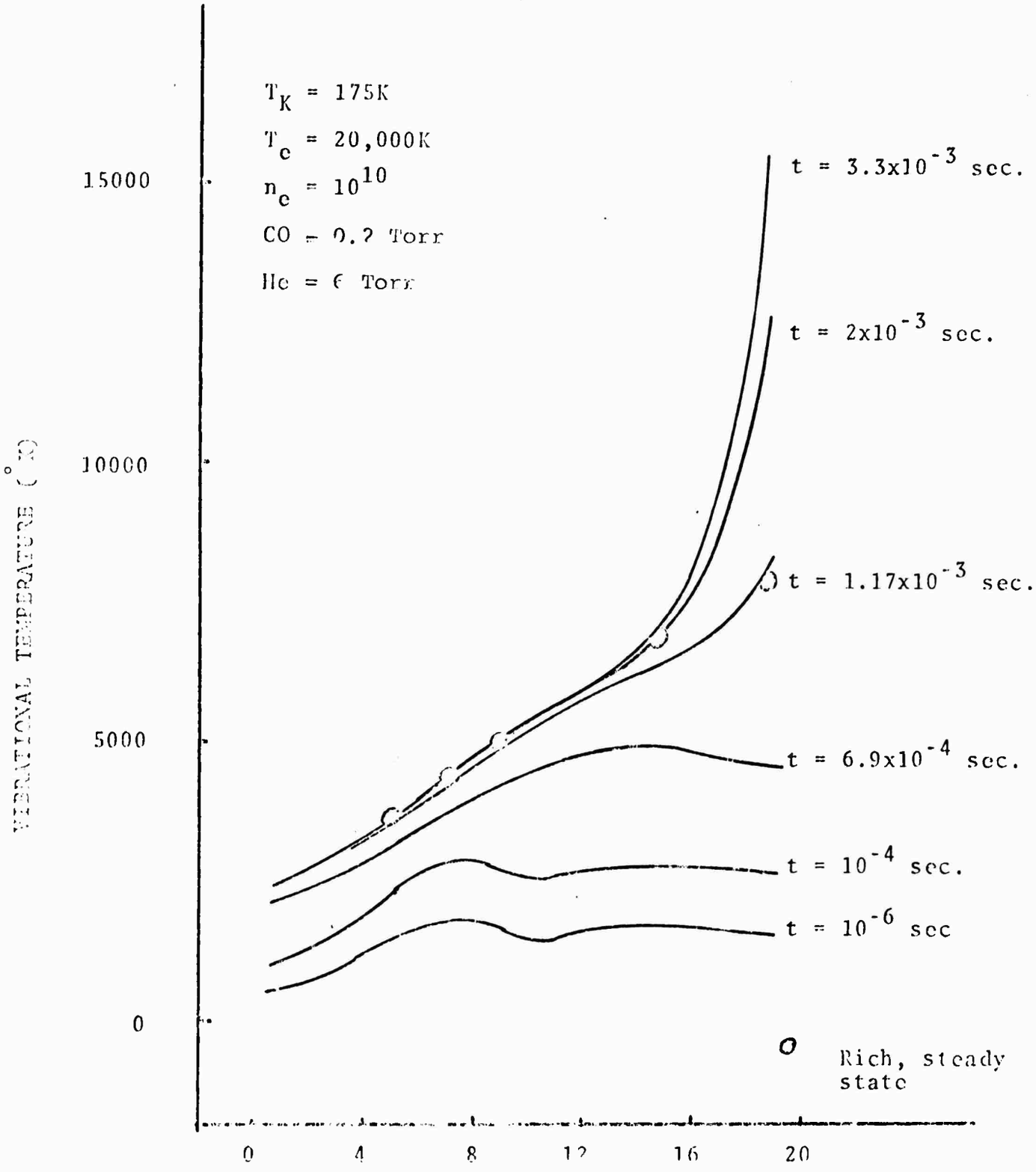

Figure 7

tions at 20. A 30 level set gives identical results for the lower levels but shifts the population to higher levels than shown in Figure 7. This effect is under current study as it appears a numerical result rather than one which is physically expected.

The circle points in Figure 7 correspond to a steady state analysis performed by Rich[26]. The agreement over the entire range is obtained in the code with increased vibrational levels.

The laser code has also been run with concentrations of N_2 present but the effect on the time development of the CO vibrational distribution is small for concentrations of N_2 equal to or less than those used for CO due to the decreased electron-vibrational rate coefficients for N_2. This particular effect will be further quantified in continued numerical studies.

Lastly, a subroutine is currently being debugged which will provide an artificial spectrum of the time developing CO vibrational distribution for direct comparison to time resolved side-light measurements on a CO-N_2-He molecular laser. The initial phases of this experimental program are outlined in the following section.

BIBLIOGRAPHY

1. K. F. Herzfeld and T. A. Litovitz, Absorption and Dispersion of Ultrasonic Waves, Academic Press, New York (1959).

2. R. C. Millikan and D. R. White, J. Chem. Phys. 39 3209 (1963).

3. R. C. Millikan and D. R. White, AIAA Journal, 2, 1844 (1964).

4. E. R. Fisher and R. H. Kummler, J. Chem Phys. 49, 1075, 1085 (1968).

5. J. H. Kiefer and R. W. Lutz, 11th International Symposium on Combustion (1966).

6. R. C. Millikan and D. R. White, J. Chem. Phys. 39, 98 (1963).

7. C. Treanor, Cornell Aero. Report AF-2184-A-1, October (1966).

8. K. E. Shuler, J. Chem. Phys. 32, 1692 (1960).

9. J. Rich and R. Rehm, Cornell Aero. Report AF-2022-A-2, May (1967).

10. E. R. Fisher and R. H. Kummler, General Electric TIS Report TIS/R67SD35, March (1967).

11. R. H. Kummler and M. H. Bortner, General Electric TIS Report TIS/R67SD40, July (1967).

12. D. Rapp and P. Englander-Golden, J. Chem. Phys. 40, 573, 3120 (1964).

13. T. E.Sharp and D. Rapp, J. Chem. Phys. 43, 1233 (1965).

14. T. Keneshea, Air Force Cambridge Research Lab. Report AFCRL-67-0221, Environmental Paper No. 263, April (1967).

15. S. H. Bauer and E. Ossa, J. Chem. Phys. 45, 434 (1966).

16. S. H. Bauer et al., Am. Chem. Soc. 160th Metting, C Chicago. Stptember (1970), Physical Chemistry Division, Abst. #70.

17. Karplus, et al., J. Amer. Chem. Soc. 89, 564 (1967).

18. J.H. Kiefer, J. Chem. Phys. 48, 2332 (1968).

19. S.H. Bauer, and E.R. Fisher, manuscript in preparation (1971).

20. G.J. Schulz, J. Phys. Rev. 135, A988 (1964).

21. J.C.Y. Chen, Chem. Phys. 40, 3513 (1964).

22. G. Abraham and E.R. Fisher, Research Institute for Engineering Sciences Report 71-31, Wayne State University, Detroit, Michigan, March (1971).

23. M. Erhardt and K.Z. Willman, Phys. Rev. 204, 462(1967).

24. L.A. Young and W.J. Eachus, J. Chem. Phys., 44, 4195 (1966).

25. W. Nighan and J.H. Bennett, Applied Phys. Letters, 14, 240(1969).

26. J.W. Rich, Applied Optics, in print (1971).

IV. Experimental Facilities

The CO laser exhibits a tremendous diversity of operating characteristics. Laser action occurs either pulsed[1] or CW[2], at liquid N_2 temperature[3], dry ice temperature[4], or room temperature[5]. Laser emission has been observed on transitions from v = 4 to v = 3, at 4.9 μm, to v = 16 to v = 15, at 5.7 μm. In general, the addition of various heavy gases, such as Hg or Xe, can increase the efficiency of laser operation.

In order to monitor the energy transfer processes in a mixture of CO, N_2, He, O_2 and other additives, an experimental facility has been constructed as follows. An optical cavity has been designed, consisting of two gold-coated mirrors, one flat, and one with a 4 meter radius of curvature. A one mm hole was drilled in the curved mirror for output coupling.

A one-meter long, pyrex tube was constructed with four viewing ports equally spaced along the upper surface, 20 cm apart. A NaCl window is secured to each viewing port. The entire discharge tube is enclosed in a plexiglass cooling enclosure. The design of the system is such that an IRTRAN lens of f/2 focal ratio can be used for viewing the spontaneous emission from the discharge.

At each end of the tube are end assemblies consisting of cylindrical, hollow copper electrodes, and Brewster-angled NaCl windows. A 20kv, 50mA power supply is used to excite the tube, either pulsed or CW.

Emission spectra are recorded using a Jarrell-Ash one-quarter meter infrared monochromator, and either a lead selenide or liquid-N_2 cooled Hg-doped, germanium detector, depending on the spectral range of observation. For CW observation, a PAR chopper and lock-in amplifier are used to provide phase-sensitive detection.

Synthetic spectra are being generated by computation to guide the identification of discharge conditions. An improved power supply has been ordered along with a coherent radiation model 201 power meter, to augment the laboratory capability.

A gas-handling system capable of feeding up to 4 gases into the laser tube simulatneously has been constructed. Flow rates are monitored for each gas with individual rotometer readings. The total gas pressure in the discharge tube is continually monitored.

In summary, a flexible experimental facility has been designed and constructed for the observation of both spontaneous and stimulated emission from gas mixtures relevant to CO laser operation, under a variety of excitation conditions. Survey spectra have been taken, and synthetic spectra are being generated for identification of discharge conditions.

References

1. C. K. N. Patel and R. J. Kerl, Appl. Phys. Letters 5, 81 (1964)

2. C. K. N. Patel, Appl. Phys. Letters 7, 246 (1965)

3. W. C. Eppers, Jr., R. M. Osgood, Jr., P. R. Greason, IEEE J. Q. E. 6, 4 (1970)

4. W. J. Graham, J. Kershenstein, J. T. Jensen, Jr., K. Kershenstein, Appl. Phys. Letters 17, 194 (1970)

5. M. M. Mann, M. L. Bhaumik, and W. B. Lacina, Appl. Phys. Letters 16, 430 (1970)

Appendix 1

VIBRATION - VIBRATION RATE COEFFICIENTS

Following Rapp (A1) we consider the following model.

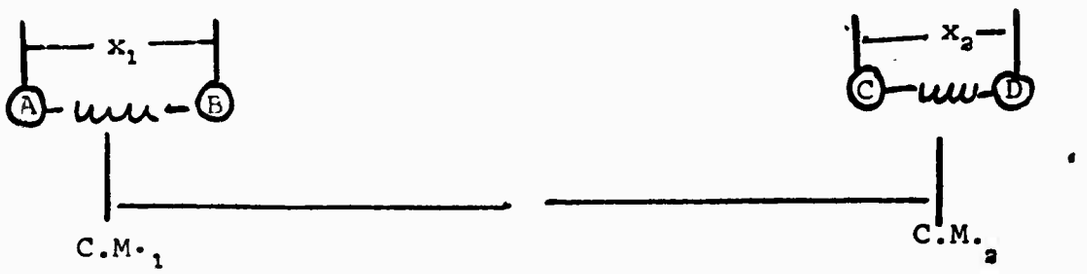

We define

$\psi_r^{AB}(x_1)$ = wave function of molecule AB in vib. state r.

$\psi_s^{CD}(x_2)$ = wave function of molecule CD in vib. state s.

The total wave function for the system of two interacting molecules can be written as an expansion in the time dependent wave functions for each molecule.

$$(1) \quad \psi = \sum_{r,s} C_{r,s}(+)\,\psi_r^{AB}(x_1)\,\psi_s^{CD}(x_2)\; e^{-i\omega_r t}\; e^{-i\Omega_s t}$$

where $\omega_r = \frac{E_r}{\hbar}$ and $\Omega_s = \frac{E_s}{\hbar}$

We set the initial conditions as the following:

$$\psi_r^{AB}(x_1) = \psi_p^{AB}(x_1) \text{ and } \psi_s^{CD}(x_2) = \psi_q^{CD}(x_2) \text{ as } t \to -\infty$$

therefore $\left|C_{pq}(-\infty)\right|^2 = 1$ and $C_{rs}(-\infty) = 0$ for $r \pm p$ and $s \pm q$.

We are now interested in solving the Schrodinger equation for the coefficient $C_{rs}(+\infty)$. The Hamiltonian is written

(2) $$H = H^{AB}(x_1) + H^{CD}(x_2) + V(y, x_1, x_2)$$

where

$H^{AB}(x_1)$ = Hamiltonian for the isolated AB diatomic,

$H^{CD}(x_2)$ = Hamiltonian for the isolated CD diatomic,

$V(y, x_1, x_2)$ = Interaction perturbation.

The assumption is now made that the interaction is exponentially repulsive in the distance B-C, and the result obtained (see Rapp and Sharp (A1)) is

(3) $$V(Y, X_1, X_2) = E_o \exp\left\{-\frac{1}{L}\left[Y - \left\{\frac{M_A}{M_A+M_B}\right\} X_1 - \left\{\frac{M_D}{M_D+M_C}\right\} X_2\right]\right\}.$$

We note that this form allows the interaction energy to be written as

(4) $$V(Y, X_1, X_2) = V(Y)V(X_1)V(X_2)$$

where

$V(Y)$ is determined from the classical trajectory of the relative motion and

$$Y = y - y_T \ , \ X_1 = x_1 - x_{1T} \ , \ X_2 = x_2 - x_{2T}$$

where the $_T$ subscripted variables represent turning point variables.

When the classical equation of motion is used (A2), one gets

$$V(Y) = E_o \ \mathrm{sech}^2 \left\{\frac{v_o t}{2L}\right\}$$

where

$$E_o = \tfrac{1}{2}\mu v_o^2 \qquad \text{and} \qquad \mu = \frac{M_{AB}\ M_{CD}}{M_{AB} + M_{CD}} \ .$$

Inserting the potential into the Schrodinger equation, multiplying by $\psi_n^{AB}(x_1)$, $\psi_s^{CD}(x_2)$ and integrating over x_1 and x_2 we find

$$\dot{C}_{ns}(t) = (\hbar i)^{-1} \ E_o \ \mathrm{sech}^2 \left\{\frac{v_o t}{2L}\right\} \sum_{r,s} C_{rs}(t) e^{i(\omega_n - \omega_r)t} \ e^{i(\Omega_s - \Omega_s)t} \cdot U_{rn} U_{sn} \tag{6}$$

where

$$U_{rn} = \int_{-\infty}^{\infty} \psi_r^{AB}(x_1) V(x_1) \psi_n^{AB}(x_1) dx_1 \ , \ \text{etc.} \tag{7}$$

We now use the 2-state approximation and arrive at the coupled equations of Rosen-Zener (A1, A3).

$$\dot{C}_1 = ife^{-2\pi i \Delta v t} C_2$$

$$\dot{C}_2 = ife^{+2\pi i \Delta v t} C_1$$

which has as a solution

$$\left|C_1(\infty)\right|^2 = \sin^2 A \ \mathrm{sech}^2(\pi \Delta v \tau) \tag{8}$$

where

$$A = \int_{-\infty}^{\infty} f(t) dt$$

and

$$f(t) = \frac{E_o}{\hbar} \ U_{rn} U_{sn} \int_{-\infty}^{\infty} \mathrm{sech}\left(\frac{2\pi v_o t}{8L}\right) dt \ .$$

This can be further reduced and integrated to give

$$f(t) = \frac{4LE_o}{\pi v_o \hbar} U_{rn} U_{sm} \int_{-\infty}^{\infty} \mathrm{sech}(x)\, dx$$

$$= \frac{4LE_o}{v_o \hbar} U_{rn} U_{sm}$$

and therefore

$$A = \frac{4\pi\mu L v_o}{h} U_{rn} U_{sm} . \tag{9}$$

Inserting this into (8), we obtain

$$P^{rn}_{sm}(v) = \sin^2\left\{\frac{4\pi L v_o}{h} U_{rn} U_{sm}\right\} \mathrm{sech}^2\left\{\frac{2LE_d}{v_o}\right\} \tag{10}$$

where

μ = reduced collision mass

L = exponential parameter

E_d = energy defect

v_o = relative velocity

h = Planck's constant

and $P^{rn}_{sm}(v)$ = velocity dependent probability for vibrational exchange from r→n and s→m.

We now consider two limits on (10), the case of large energy defect and small energy defect. First we note for essentially all cases of interest

$$\sin^2\left(\frac{4\pi\mu L v_o}{h} U_{rn} U_{sm}\right) \cong \frac{16\pi^2\mu^2 L^2 v_o^2}{h^2} U^2_{rn} U^2_{sm} . \tag{11}$$

And, for the case of large energy defect

$$\mathrm{sech}^2\left(\frac{2LE_d}{v_o}\right) \cong 4 \exp\left(-\frac{4LE_d}{v_o}\right) \tag{12}$$

and for the case of small energy defect

$$\text{(13)} \qquad \operatorname{sech}^2\left(\frac{2LE_d}{v_o}\right) \cong 1 - \frac{4L^2E_d^2}{v_o^2} \,.$$

The rate coefficient for vibration-vibration exchange processes can be obtained from (10) by integrating over the collision frequency and the one-dimensional velocity distribution. Thus,

$$\text{(14)} \qquad R^{r\,n}_{s\,m}(T) = \int_0^\infty P^{r\,n}_{s\,m}(v_o)\ \Gamma(v_o) f(v_o)\, dv_o$$

where $\Gamma(v_o)$ = hard sphere collision frequency

$$= \pi\sigma^2 v_o$$

and $f(v_o)$ = Boltzmann velocity distribution

$$= \left(\frac{\mu}{kT}\right) v_o \quad \exp\left\{\frac{-\mu v_o^2}{2kT}\right\}$$

with σ = hard sphere collision diameter.

Considering the case of small energy defects, (14) becomes

$$\text{(15)} \qquad R^{r\,n}_{s\,m}\Big|_{S.E.D.L.} = \frac{16\pi^2\mu^2L^2U^2_{r\,n}U^2_{s\,m}}{h^2}\left(\frac{\mu}{kT}\right)\ \pi\sigma^2\ I(T)$$

where $I(T)$ is the following integral

$$\text{(16)} \qquad I(T) = \int_0^\infty v_o^4\left(1 - \frac{4L^2Ed^2}{v_o^2}\right)\exp\left\{\frac{\mu v_o^2}{2kT}\right\} dv_o$$

$$= I_1(T) - I_2(T)$$

where

$$I_1(T) = \int_0^\infty v_o^4\ \exp\left\{\frac{-\mu v_o^2}{2kT}\right\} dv_o$$

and

$$I_2(T) = 4L^2E_d^2 \int_0^\infty v_o^2 \exp\left\{\frac{uv_o^2}{2kT}\right\} dv_o \ .$$

The integrals in (16) are both of the form

$$(17) \qquad \int_0^\infty x^{2n} \exp\left\{-ax^2\right\} dx = \frac{1\cdot3\cdot5\cdots(2n-1)}{2^{n+1}\ a^n} \sqrt{\frac{\pi}{a}},$$

Therefore,

$$(18) \qquad I_1(T) = \frac{3\sqrt{2}}{2}\ \pi^{\frac{1}{2}} \left(\frac{kT}{\mu}\right)^{\frac{5}{2}}$$

and

$$(19) \qquad I_2(T) = 2\sqrt{2}\ \pi^{\frac{1}{2}} L^2 E_d^2 \left(\frac{kT}{\mu}\right)^{3/2}$$

If we substitute (18) and (19) into (15) we obtain the small energy defect rate coefficient

$$(20) \qquad R_{sm}^{rn}\Big|_{S.E.D.L.} = \frac{24\sqrt{2}}{h^2}\ \pi^{7/2}\ \mu^{\frac{1}{2}}\ L^2\ \sigma^2 (kT)^{3/2}\ U_{rn}^2\ U_{sm}^2 \left[1 - \frac{4\mu L^2 E_d^2}{3kT}\right].$$

This rate coefficient can be simplified into convenient units through the following substitutions:

$$\mu^{\frac{1}{2}} = \mu_M^{\frac{1}{2}} \left(\frac{1}{6.02^{23}}\right)^{\frac{1}{2}} = \mu_M^{\frac{1}{2}}\ (1.289^{-12})$$

$$L^2 = L_A^2 \quad (1^{-16})$$

$$\sigma^2 = \sigma_A^2 \quad (1^{-16})$$

therefore,

$$R_{gn}^{rn}\Big|_{S.E.D.L.} = 8.88^{-14}\ \mu_M^{\frac{1}{2}}\ L_A^2\ \sigma_A^2\ T^{3}{}_{2}\ U_{rn}^2\ U_{gn}^2\ \left[1 - \frac{4\mu L^2 E_d^2}{3kT}\right]$$

and

$$\frac{4\mu L^2 E_d^2}{3kT} = 5.703^{-3}\ \left[\frac{\mu_M L_A^2\ E_d^{-2}}{T}\right]$$

where $\bar{E}_d$ is in cm^{-1}

The small energy defect rate coefficient then becomes

$$R_{gn}^{rn}\Big|_{S.E.D.L.} = 8.88^{-13}\ \mu_M^{\frac{1}{2}}\ L_A^2\ \sigma_A^2\ T^{3}{}_{2}\ U_{rn}^2\ U_{gn}^2\ \left[1 - 5.703^{-3}\ \frac{\mu_M L_A^2 \bar{E}_d^{-2}}{T}\right] \tag{22}$$

The large energy defect rate coefficient can be similarly evaluated as follows. If (11) and (12) is inserted into (14) we obtain

$$R_{gn}^{rn}\Big|_{L.E.D.L.} = \frac{16\pi^2\mu^2 L^2}{h^2}\ U_{rn}^2\ U_{gn}^2\ 4\pi\sigma^2 \left(\frac{\mu}{kT}\right) I_o\ (T) \tag{23}$$

where

$$I_o(T) = \int_o^\infty v_o^4\ \exp\left\{\frac{-\mu v_o^2}{2kT} - \frac{4LE_d}{v_o}\right\} dv_o\ . \tag{24}$$

The integral in (23) cannot be evaluated in closed form but it is standard for this type of integral (A4) to expand about the maximum of the exponent.

The maximum of the exponent is obtained as

$$\frac{d}{dv_o} \left\{ \frac{-\mu v_o^2}{2kT} - \frac{4LE_d}{v_o} \right\} = 0$$

which leads to

$$v_M = \left(\frac{4LE_d kT}{\mu} \right)^{1/3}$$

Expanding the kernal in the integral $I_o(T)$ about v_M we obtain

$$K_o(v_o) = K_o(v_M) + \frac{(v_o - v_M)^2}{2} \left. \frac{\partial^2 K_o}{\partial v_o^2} \right|_{v_M} + H.O.T. \tag{25}$$

The second derivations in (25) can be evaluated as

$$\left. \frac{\partial^2 K_o}{\partial v_o^2} \right|_{v_M} = -\frac{\mu}{kT} - \frac{8LE_d}{V_M^3} \tag{26}$$

which upon substitution of v_M gives

$$\left. \frac{\partial^2 K_o}{\partial v_o^2} \right|_{v_M} = \frac{-3\mu}{kT}$$

Substituting (26) and (25) into (24) yields

(27) $$I_o(T) = \int_0^\infty v_o^4 \exp\left\{\frac{-\mu v_M^2}{2kT} - \frac{4LE_d}{v_M}\right\} \exp\left\{-\frac{3\mu}{kT}\frac{(v_o - v_M)^2}{2}\right\} dv_o \ .$$

This integral is now of a standard form and can be integrated to give (upon extension of limits)

(28) $$I_o(T) = v_M^4 \exp\left\{\frac{-\mu v_M^3 - 8kTLE_d}{2kTv_M}\right\} \left(\frac{4\pi kT}{3\mu}\right)^{\frac{1}{2}} \ .$$

The exponential function in (28) can be simplified via v_M to give

$$\exp\left\{\frac{-\mu v_M^3 - 8kTLE_d}{2kTv_M}\right\} = \exp\left\{-6\left(\frac{\mu}{kT}\right)^{\frac{1}{2}}\frac{LE_d}{2}\right\}^{2/3}$$

Assembling (29),(28), into (23) we obtain

(29) $$R_{\theta\theta}^{rr}\Big|_{L.E.D.L.} = \frac{64\pi^3\mu^2}{h^2} L^2\sigma^2 U_{rn}^2 U_{\theta n}^2 \left(\frac{\mu}{kT}\right) v_M^4 \left(\frac{4\pi kT}{3\mu}\right)^{\frac{1}{2}}$$

$$\cdot \exp\left\{-6\left(\frac{\mu}{kT}\right)^{\frac{1}{2}}\left(\frac{LE_d}{2}\right)\right\}^{2/3} \ .$$

which upon inserting the expression for v_M^4 gives

(30) $$R_{\theta\theta}^{rr}\Big|_{L.E.D.L.} = 64\left(\frac{4}{3}\right)^{\frac{1}{2}}(4)^{4/3}\frac{\pi^{7/2}\mu^{7/6}}{h^2} k^{5/6} L^{10/3} T^{5/6} \sigma^2 E_d^{4/3} U_{rn}^2 U_{\theta n}^2$$

$$\cdot \exp\left\{-6\left(\frac{\mu}{kT}\right)^{\frac{1}{2}}\left(\frac{LE_d}{2}\right)^{2/3}\right\} \ .$$

The pre-exponential factor can be reduced to convenient units via

$$\mu^{7/6} = \mu_M^{7/6} \left[\frac{1}{6.02^{23}}\right]^{7/6} = 1.81^{-28}\ \mu_M^{7/6}$$

$$L^{10/3} = L_A^{10/3}\ (1^{-8})^{10/3} = 2.14^{-27} L_A^{10/3}$$

$$\sigma^2 = \sigma_A^2 (1^{-16})$$

and

$$E_d^{4/3} = E_d^{-4/3} (2\pi c)^{4/3} = 1.09^{15} E_d^{-4/3}$$

and where

$$k^{5/6} = 6.08^{-14}$$

yielding

$$= 1.508^{-12} T^{5/6}\ \mu_M^{7/6}\ L_A^{10/3}\ \sigma_A^2\ E_d^{4/3}\ U_{rn}^2\ U_{sm}^2 \quad .$$

And the exponent can be reduced similarly to yield

$$\left(\frac{LE_d}{2}\right)^{2/3} = 96.1\ (L_A \overline{E}_d)^{2/3}$$

$$\left(\frac{\mu}{kT}\right)^{1/3} = 2.29^{-3} \left(\frac{\mu_M}{T}\right)^{1/3}$$

Thus, the exponent becomes

$$-1.32\ (L_A \overline{E}_d)^{2/3} \left(\frac{\mu_M}{T}\right)^{1/3} \quad .$$

Inserting the pre-exponential and the exponential factor in (30) gives

$$(31) \qquad R^{r\,n}_{s\,s}\Big|_{L.E.D.L.} = 1.508^{-12}\ \mu_M^{7/6} L_A^{10/3}\ \sigma_A^2\ \overline{E}_d^{4/3}\ U_{r\,n}^2\ U_{s\,s}^2\ T^{5/3}$$

$$\cdot\left\{\exp -1.32\ (L_A \overline{E}_d)^{2/3} \left(\frac{\mu_M}{T}\right)^{1/3}\right\}$$

Thus, (22) and (31) are the rate coefficients for vibration-vibration exchange processes in the small energy defect and large energy defect limits, respectively. The units for these coefficients can be listed as follows

μ_M = reduced mass in molecular units

L_A = exponential parameter in Å.

σ_A = hard sphere diameter in Å.

T = temperature in °K

$\overline{E}_d$ = energy defect in cm^{-1}

and

$U_{r\,n}$ = matrix element for r→n vibrational transition.

Appendix II

FUNDAMENTAL MOLECULAR PROCESSES IN CARBON MONOXIDE LASER SYSTEMS

E. R. Fisher

and

R. H. Kummler

Department of Chemical Engineering and Material Sciences

Invited paper presented at the Conference on Laser Physics, Sun Valley, Idaho, March 1-3, 1971.

B

FUNDAMENTAL MOLECULAR PROCESSES IN CO LASER SYSTEMS

I. Introduction

Despite some of its own idiosyncrasies (partial inversion, multilevel action) the CO laser has appeared to be a tantalizingly straight forward application of known atomic and molecular processes which in most cases have been theoretically and experimentally very thoroughly documented in recent years. Indeed, optimism appears to be reasonably justified in view of the large expertise developed for analysis of more complex reentry and upper atmospheric problems which involve large sets of relaxing vibrational modes in diatomics[1-3]. Early results for CO and CO/N_2 systems[4] are encouraging, although experimental results involving the effects of minor additives such as Hg addition[5-7] need increased study for inclusion into models for molecular laser behavior.

Fundamental processes worthy of consideration are shown in Figure 1. Only those processes which create the laser action and not those which destroy it, are included. Other processes which must be considered in a more complete treatment of this system would include ionization of CO to form CO^+, followed by dissociative recombination:

$$CO^+ + e \rightarrow C + O$$

which would lead to carbon deposits and presumably eventual depletion of the CO over long term operation. Although the

Figure 1

FUNDAMENTAL MOLECULAR PROCESSES IN CO

LASER SYSTEMS

1. ELECTRON IMPACT EXCITATION

$$e + CO \rightarrow \{CO^-\} \rightarrow CO^{\ddagger} + e$$

$$e + Hg \rightarrow Hg^* + e$$

2. ELECTRON IMPACT IONIZATION

$$e + Hg \rightarrow Hg^+ + 2e$$

3. ELECTRONIC - VIBRATIONAL ENERGY TRANSFER

$$Hg^* + CO \rightarrow Hg + CO^{\ddagger}$$

4. VIBRATION VIBRATION ENERGY EXCHANGE

$$N_2(v) + CO(r) \rightarrow N_2(v-1) + CO(r+1)$$

5. VIBRATION-TRANSLATION ENERGY TRANSFER

$$CO(r) + He \rightarrow CO(r-1) + He$$

6. RADIATIVE PROCESSES

Spontaneous

Induced

rate constants for this particular reaction are not at present known, analogous reactions for NO^+, N_2^+, O_2^+, etc. are well established[8]. The cross section data for electron impact excitation of both diatomics[9] and atoms[10] has been available for some time and recently, the rate constants for such processes in N_2 and CO have been documented[11].

In the case of Hg, or any low ionizaiton potential additive, an important result of the ionization step could be additional electrons with a resulting electron temperature decrease due to the thermalization of the hot electrons by the near thermal electrons produced in the Hg ionization. If one examines the limiting case of Hg^+ equilibrium with the electron temperature through the Saha equation, it is highly probable at T_e = 20,000°K that most of the Hg will be ionized. At a vapor pressure of Hg, of 1μ, this could represent 10^{13} electrons/cc as an upper limit. The remaining Hg (or Xe) which is not ionized will be excited electronically, and despite the fact that the radiative lifetime of Hg (^3P) is 10^{-7} sec, radiation trapping will cause substantial quenching by CO or N_2 with resultant conversion of electronic energy to vibrational energy.

Electron Impact Processes

Consider first the excitation of N_2 by electron impact. Because this process proceeds through an unstable negative ion intermediate state, there is an activation energy for the process which leads to a threshold of about 1.5 ev rather than the

0.29 ev vibrational spacing. Cross sections are large for collision energies between 2 and 4 ev, approaching gas kinetic at the maximum, for excitation from the ground vibrational level to levels from 1 through 8 as shown in Figure 2. Beyond 6 or 7, the cross sections diminish rapidly and are therefore of little importance compared to excitation from excited vibrational levels to still higher levels as will be seen.

Similar data exist for CO as shown in Figure 3. It is significant that the threshold for CO excitation occurs below 1 ev and that the cross sections are four times as large for CO as for N_2 excitation.

Aside from putting energy into the vibrational mode, the implications of these electron impact processes are illustrated in Figure 4, from Nighan's work[12]. The electron energy (u) distribution $f(u) = 2 \frac{1}{\sqrt{\pi}} T_e^{-3/2} e^{-u/T_e}$ would be a straight line if the distribution were Maxwellian. The large deviations from a straight line, characterized by the absence of electrons with energy greater than about 2 ev for N_2 is the result of the large vibrational excitation cross sections which provides an energy loss mechanism nearly preventing electrons from reaching energies above 2 ev.

However, as T_v increases the reverse mechanism rebuilds part of the distribution, and this tail may in fact be important for electronic and ionization processes.

However, because we are interested in rate constants or integrated cross sections, we need not worry about deviations

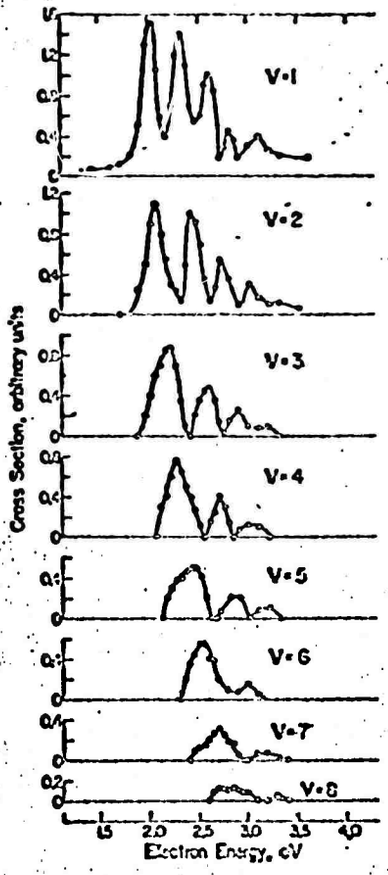

Fig. 2 Energy dependence of the vibrational cross section of nitrogen by electron impact. The curves are obtained from sets of curves similar to Fig. 3 taken at different energies of the incident electrons. When the ordinate numbers are multiplied by 10^{-16} a cross-section scale (in cm^2) is obtained such as to give a total vibrational cross section in agreement with Haas. See text for a discussion of errors in cross-section scale.

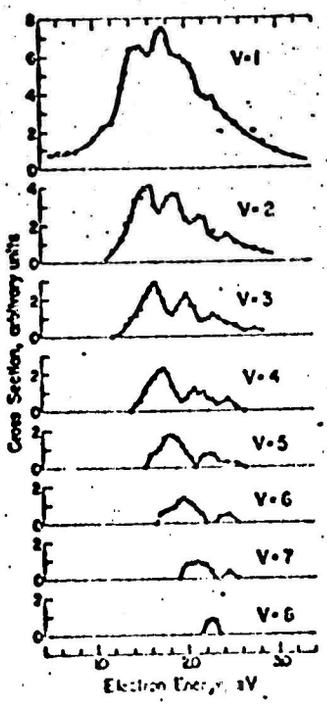

Fig. 3 Energy dependence of the vibrational cross section of CO to the first eight vibrational states. Analogous to Fig. 2

Figure 4

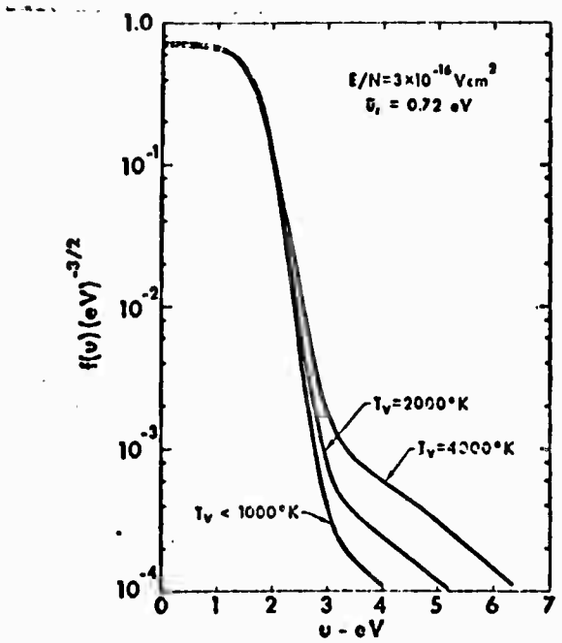

Fig. 4. Electron energy distribution functions in N_2 calculated for various vibrational temperatures.

from a Boltzmann distribution for vibrational excitation as illustrated in Figure 5. Rate constants for N_2 excitation are insensitive to the electron kinetic temperature above 1 ev or 11,000°K. At this point, the rate constants are very large. It is especially interesting to note the comparison between $k_{0,4}$ and $k_{0,8}$ which at high T_e are very nearly equal. Thus, at high vibrational temperatures a two step process may be the preferred electron excitation route. Again, the tail of the electron distribution is much more important in exciting electronic states of additives than for increasing the vibrational excitation rates.

Quenching of Electronic States by Molecules

Once an additive atomic species has been electronically excited, there is the possibilities of energy transfer to the vibrational mode depending upon the potential energy curves of the system quenching system. Two types of quenching mechanisms are shown in Figure 6. First is the ionic intermediate mechanism, which is the preferred route for the quenching of excited electronic states of low ($\tilde{<}$ 4 ev) ionization potential atomic species such as the alkali atoms, by diatomic molecules, two important examples of which are N_2 and CO. The second is a covalent mechanism which proceeds directly through a curve crossing mechanism involving the direct crossing of reactant excited state of a stable or metastable intermediate and product potential curves. An example of this type is the quenching of $O(^1D)$ by N_2 (reference 15).

Figure 5

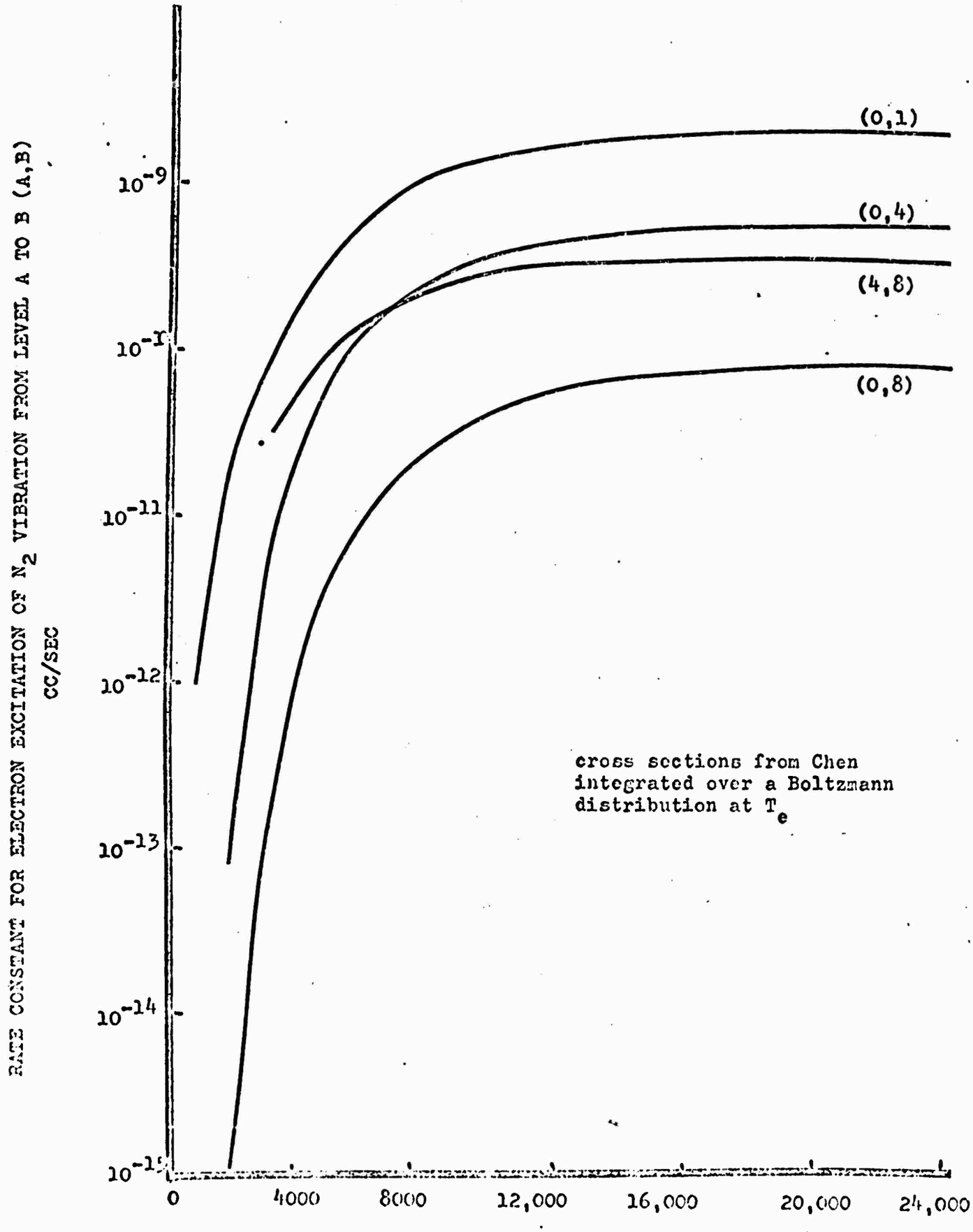
RATE CONSTANT FOR ELECTRON EXCITATION OF N_2 VIBRATION FROM LEVEL A TO B (A,B)
CC/SEC
10^{-9}
10^{-11}
10^{-12}
10^{-13}
10^{-14}
(0,1)
(0,4)
(4,8)
(0,8)
cross sections from Chen integrated over a Boltzmann distribution at T_e
0
4000
8000
12,000
16,000
20,000
24,000
ELECTRON KINETIC TEMPERATURE, K

Figure 6

QUENCHING OF ELECTRONIC STATES BY MOLECULES

$$A^* + M_2 \rightarrow A + M_2$$

(a) Ionic Curve Crossings

$$Na(3^2P) + N_2 \rightarrow \{Na^+ - N_2^-\} \rightarrow Na(3^2S) + N_2(v^+)$$

(b) Covalent Curve Crossing

$$O(^1D) + N_2 \rightarrow \{N_2O\}^* \rightarrow O(^3P) + N_2$$

$$Hg(6^3P_{1,0}) + CO \rightarrow \{HgCO\}^* \rightarrow Hg(6^1S_0) + CO(v_S)$$

The principle involved in the ionic mechanism is illustrated for atom-atom quenching in Figure 7. At large interaction distances, and hence with potentially large cross sections the potential curves corresponding to the ionic intermediate complex become energetically favorable compared to the excited curve providing a curve crossing mechanism coupling initial (reactant) curves with final (product) curves. The curve crossing at each point of intersection can be independently evaluated and is assumed to be given by the Landau Zener form[13]. The transition matrix element is obtained from the electronic component (known from the Hasted Chong correlation)[14]. The vibrational overlap integral at the crossing point, which is obtained from the appropriate Franck Condon factors, is necessary to describe excited atom quenching by molecules. The potential energy curves for electronic states have superimposed on them the vibrational levels of both the diatomic and the negative ion, so that the overall partial cross sections are computed via a classical diffusion through the illustrated potential grid (Figure 8).

Sample results of Na (3^2P) quenching by N_2 are shown in Figure 9. The significant feature of the result is the non-resonant behavior and the large fractional energy which goes into vibrational (over 50%).

The potential energy curves for a covalent quenching reaction such as $O(^1D) + N_2$ are sketched in Figure 10[15]. For this case, the interaction matrix element at each crossing point is given by an electronic contribution due to spin-orbit coupling

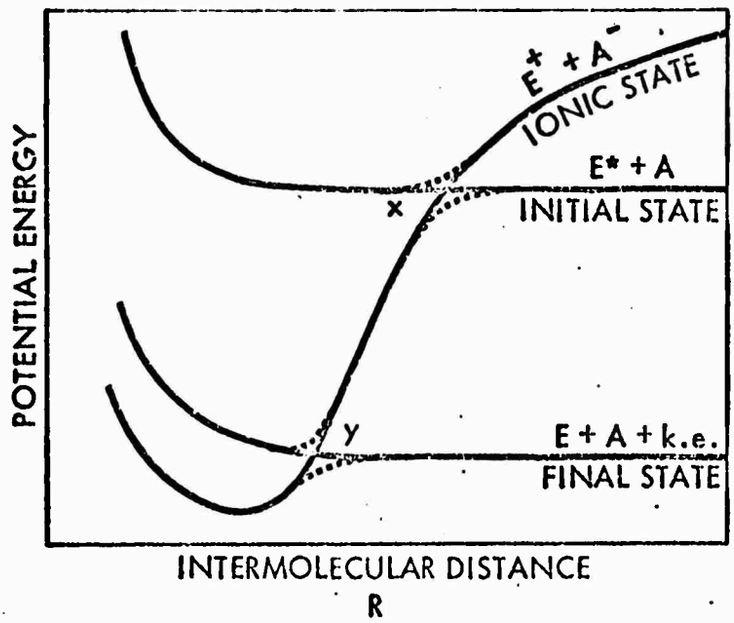

FIGURE 1. Potential Energy Curves for an Atom-Atom System

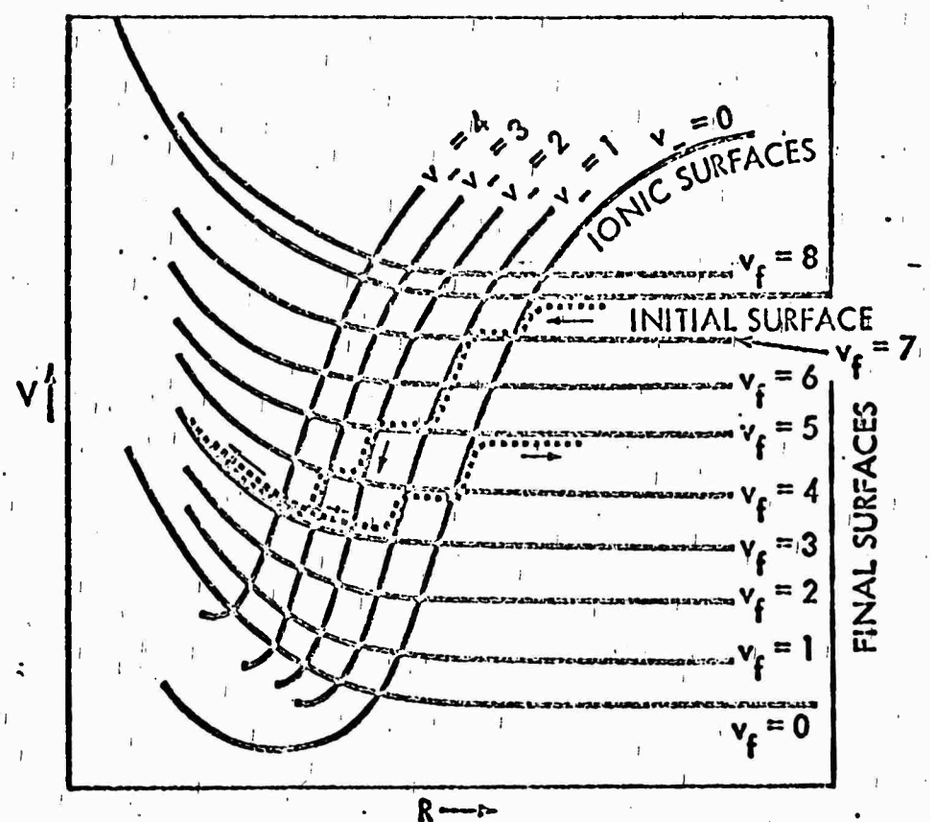

Figure 8: Simplified potential curves for an excited atom - molecule quenching reaction.

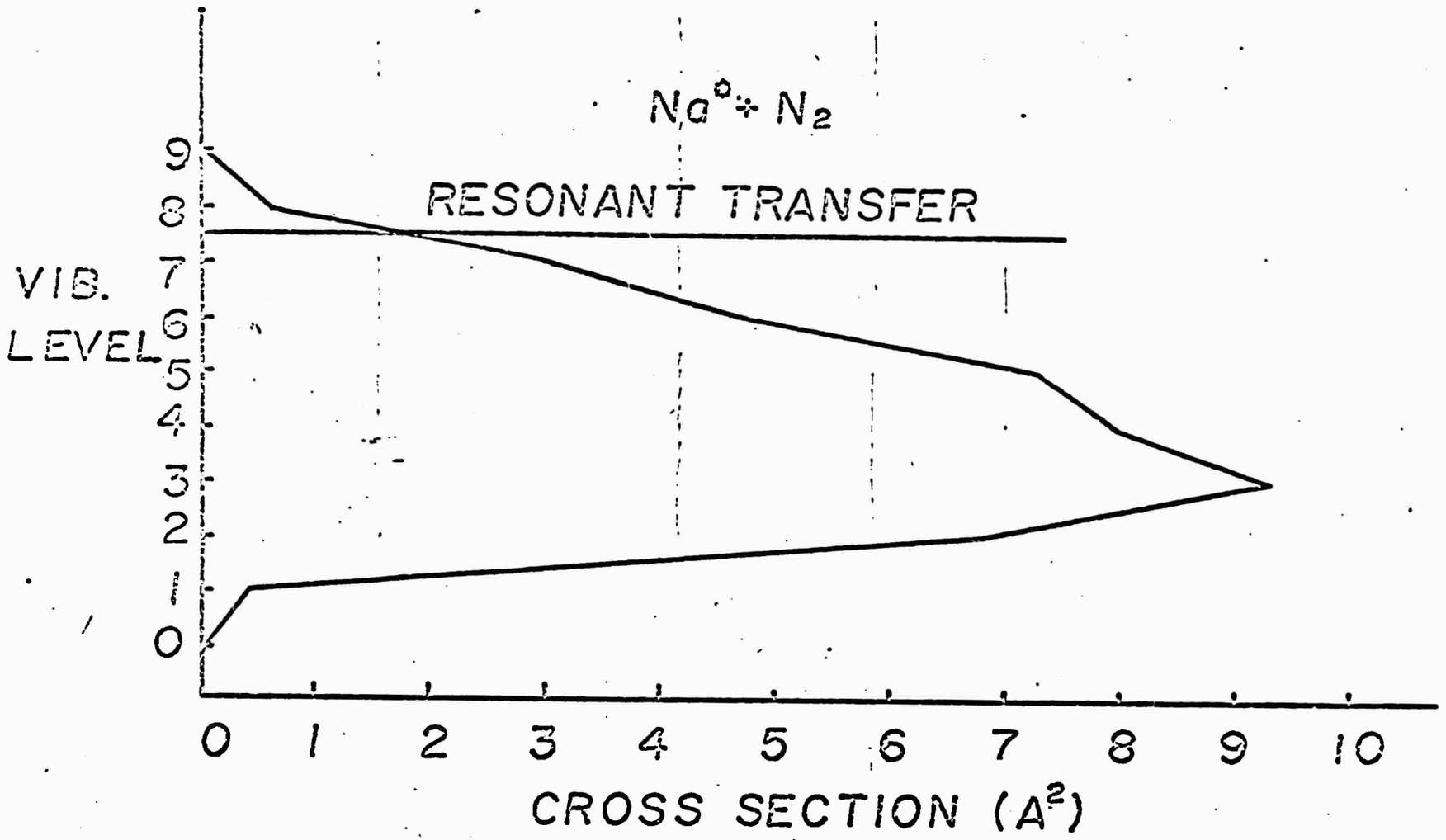

Figure 9: Partial cross sections for the $Na(3^2P) + N_2(v=0)$ reaction for an initial kinetic energy = 0.2 ev and a polarizability = 40 A^3. The calculated total cross section is 40.0 A^2.

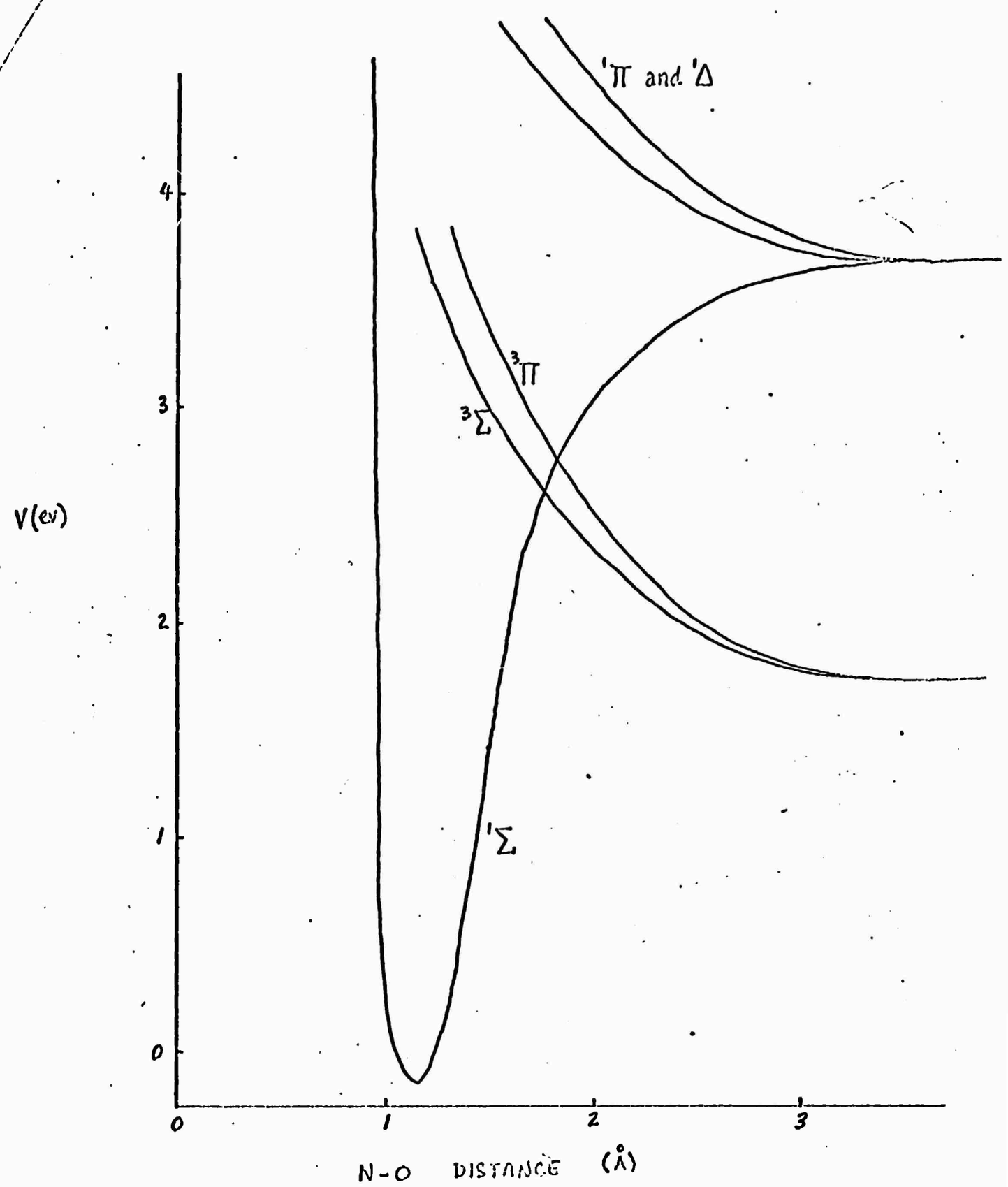

Figure 10

P.E. CURVES FOR O('D) QUENCHING BY N_2

while the vibrational overlap is to compute, to lowest order, between vibrational wave functions of the same molecule, i.e. N_2 in this case. Thus, the only quenching channels which have significant interaction elements (or cross sections) are those in which the vibrational state of the reactant N_2 is nearly unchanged. Thus, the expected vibrational excitation produced in covalent quenching reactions is small[15]. This result has been indirectly verified by recent atmospheric vibrational temperature analysis[16].

In the case of Hg quenching by CO, the potential energy curves are not available for theoretical analysis, but experimental data is available. The system is shown in Figure 11, and the experimental results of Polanyi[17] are shown in Figure 12. Even though Hg^* lifetimes are 10^{-7} sec, as shown in Figure 13, it is well known from very early studies on Hg areas that significant radiation trapping occurs under plasma conditions so that an important fraction of the electronic energy eventually channels into the vibrational mode.

Vibrational Exchange

The vibrational Master equation[1] is illustrated in Figure 14. A slowly time varying quasisteady state solution to the Master has been found by Treanor[18] to be

$$n_r = n_o \exp(-r\gamma) \exp(-E_r/kT)$$

$$\equiv n_o \exp(-E_r/k\theta_r^*),$$

Partial Quenching Cross Sections in Ang.^{2}
for $O(^1D) + N_2$ - co-linear case

triplet vibr. level	Maximum Spin-Orbit Interaction 300 cm^{-1}	500 cm^{-1}
6	0.0	0.0
5	0.0	0.0
4	0.0	0.0
3	0.0	0.0
2	0.0	0.002
1	0.0	0.33
0	2.8	5.7
total quenching cross section	2.8	6.03

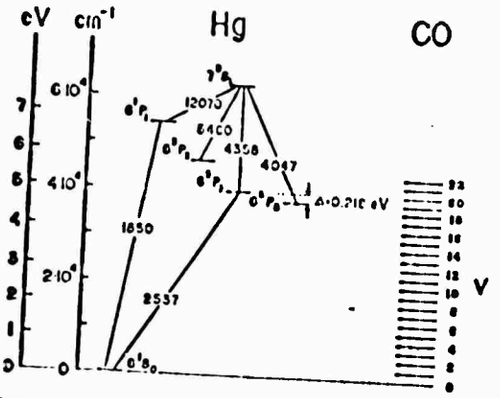

Fig. 11. Mercury levels and CO vibrational energy levels.

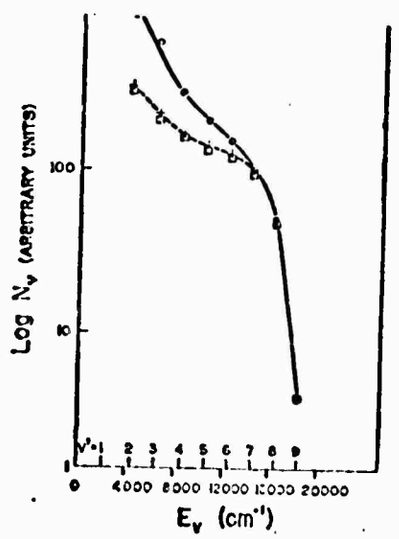

Fig. 12a

Vibrational distribution of CO, showing the effect of impurity in CO. (a) Run (1): impure CO without diluent +, (b) Run (6): impure CO with Ar □, (c) Run (2): purified CO without diluent O.

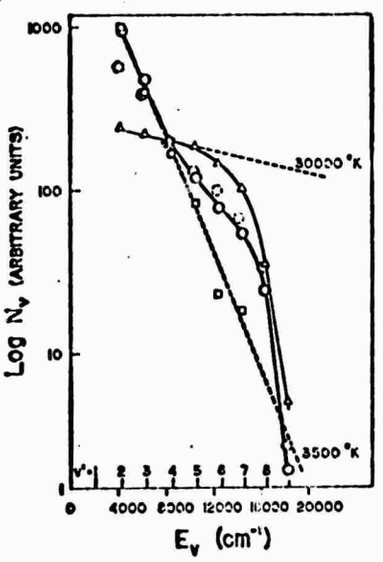

Fig. 12b

Vibrational distribution of (purified) CO, showing the effect of inert diluent with high and with normal mercury pressure, and the effect of 'vibrational scavenger'. (a) Run (4): CO in Ar, high Hg pressure, □, (b) Run (5): CO in Ar, normal Hg pressure, O, (c) Run (3): CO in N_2, normal Hg pressure, △, (d) Run (2): purified CO without diluent, dashed circle.

Fig. 13. Quenching cross sections (Å²) and radiative lifetimes (τ in seconds).[a]

Quenching gas	Electronic state: $Hg^*(6^3P_1)$ (total)	$Hg^*_1 \rightarrow Hg^*_0$	$Hg^*_1 \rightarrow Hg$	Hg^*_0 (total)
CO	4.0[b]	$\sigma_0^2 = 0.57$[b,c]	$\sigma_1^2 = 3.5$	$\sigma_0^2 = 0.028$
N_2	0.42[e]	$\sigma_0^2 = 0.42$[f]	$\sigma_1^2 \approx 0$[e]	$\sigma_0^2 = 10^{-5}$
Ar	0.223[d]	$\sigma_0^2 = 0$[b]	$\sigma_1^2 = 0.2$[d]	$\sigma_0^2 = 0$
Hg	...	...	...	$\sigma_0^2 = 7.6$
τ (sec)	1.0×10^{-7}[g]	...	1.0×10^{-7}	7.5×10^{-3}[i]

Figure 14

RELAXATION BY VIBRATION EXCHANGE.

master equation

$$\frac{dn_r}{dt} = P_{r+1,r}\left[n_{r+1}n - \exp\left(-\frac{E_{r+1}-E_r}{kT}\right)n_r n\right] - P_{r,r-1}\left[n_r n - \exp\left(-\frac{E_r-E_{r-1}}{kT}\right)n_{r-1}n\right] + \sum_s P_{r+1,s}^{r-1,s}$$

$$\times\left[n_{r+1}n_{s-1} - \exp\left(-\frac{E_{r+1}+E_{s-1}-E_r-E_s}{kT}\right)n_r n_s\right] - \sum_s P_{r,r-1}^{s,s+1}\left[n_r n_s - \exp\left(-\frac{E_r+E_s-E_{s+1}-E_{r-1}}{kT}\right)n_{s+1}n_{r-1}\right]$$

$$+Q_{r+1,r}\left[n_{r+1}N - \exp\left(-\frac{E_{r+1}-E_r}{kT}\right)n_r N\right] - Q_{r,r-1}\left[n_r N - \exp\left(-\frac{E_r-E_{r-1}}{kT}\right)n_{r-1}N\right]$$

$$+\sum_R Q_{r+1,r}^{R-1,R}\left[n_{r+1}N_{R-1} - \exp\left(-\frac{E_{r+1}+F_{R-1}-E_r-F_R}{kT}\right)n_r N_R\right]$$

$$-\sum_R Q_{r,r-1}^{R,R+1}\left[n_r N_R - \exp\left(-\frac{E_r+F_R-E_{r-1}-F_{R+1}}{kT}\right)n_{r-1}N_{R+1}\right].$$

$$N_R = N_o \exp(-R\gamma) \exp(-F_R/kT)$$

$$\equiv N_o \exp(-F_R/k\phi_R^*),$$

where it may be shown by substitution that γ is the same for both molecules, and where θ_r^* and ϕ_R^* are population factors for the rth and Rth vibrational levels of species A and B, respectively. γ may be evaluated in terms of level 1 of either molecule:

$$\gamma = (E_1/k)\ (1/\theta_1^* - T^{-1}) = (F_1/k)\ (1/\phi_1^* - T^{-1}),$$

so that

$$n_r = n_o \exp\left\{\frac{-E_r}{k\theta_1^*}\left[\frac{rE_1}{E_r} - \frac{\theta_1^*}{T}\left(\frac{rE_1}{E_r} - 1\right)\right]\right\}$$

and

$$N_R = N_o \exp\left\{-\frac{F_R}{k\phi_1^*}\left[\frac{RF_1}{F_R} - \frac{\phi_1^*}{T}\left(\frac{RF_1}{F_R} - 1\right)\right]\right\}$$

For anharmonic oscillators, these distributions are clearly non-Boltzmann since the terms in brackets are dependent on the vibrational level. In the harmonic model, $E_r = rE_1$ and $F_R = RF_1$, therefore

$$n_r = no \exp(-rE_1/k\theta_H),$$

and

$$N_R = N_o \exp(-RF_1/k\phi_H),$$

where $\theta_H \equiv \theta_1^*$ and $\phi_H \equiv \phi_1^*$, are the vibrational temperatures for species A and B, respectively. Here, we find Boltzmann distributions with the relationship between θ_H and ϕ_H given by

$$(E_1/\theta_H) - (F_1/\phi_H) = (E_1 - F_1)/T$$

Further, the relationship between populations in the same level R is

$$\frac{n_R}{N_R} = \frac{n}{N}\frac{Z}{z} \exp\left[-\frac{R(E_1 - F_1)}{kT}\right],$$

where n and N are the total concentrations and z and Z are the vibrational partition functions of species A and B, respectively, defined by

$$z = \sum_R \exp\left(-RE_1/k\theta_H\right)$$

and

$$Z = \sum_R \exp\left(-RF_1/k\phi_H\right).$$

It is important to note that the VV steady-state forces the relative distributions of the two species to be nearly characterized by the kinetic temperature even though the vibrational temperature of each species may be considerably higher than given by equilibrium. The ratio of partition function for species A and B is weakly dependent on the vibrational temperature, and thus, deviates slightly from equilibrium. This characteristic of steady-state VV exchange processes in gas mixtures in the harmonic model is also found in the anharmonic model. This is the

important pumping mechanism which creates the partial inversion in the CO laser.

In Figure 15a we show the LeGay[19] demonstration of the validity of the VV model for N_2 - CO systems. In Figure 15b, the effect of rotational temperature which will make the agreement of Figure 15a better is shown. Other verifications have been done by Cornell[20], Aerospace[21], (Figure 16), AVCO[22], etc.

A time dependent model for a pulsed CO system including all these energy transfer processes for a pure CO system of 20 levels is shown in Figure 17. The vibrational population factor or temperature for each vibrational level in a 20 level program in CO and He is shown as a function of time, as computed through the Runge Kutta Merson[1,3] integration technique including electron impact excitation for all levels, VV, VT processes and spontaneous emission. A comparison with the Rich[4] steady state calculation is shown.

A similar model describing the pulsed behavior of N_2 - CO - He in the presence of hot electrons has also been developed. The presence of N_2 plays only a small role in enhancing the CO vibrational populations unless the N_2 concentration is greater than the CO.

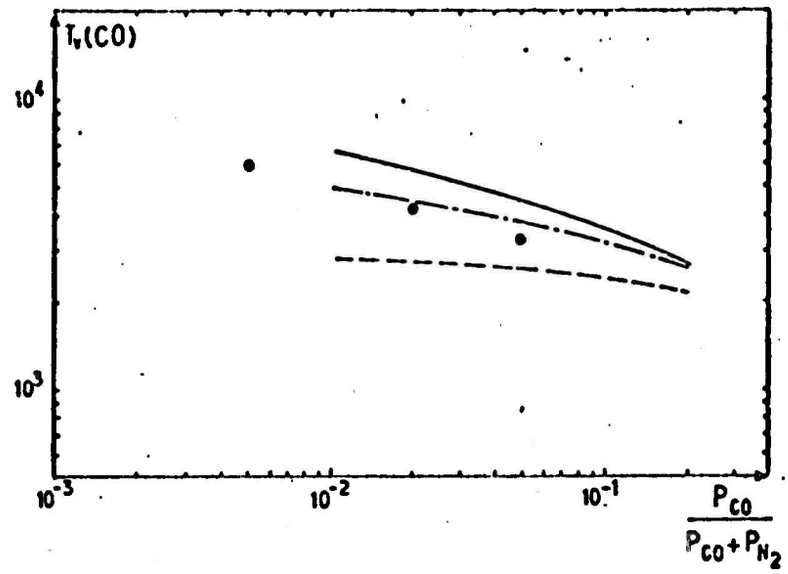

Fig. 15 a. Rearranged Boltzmann temperature vs. CO relative concentration: curves given by Fisher and Kummler (1968*b*) for $T_v^0(N_2) = 2000$ °K, kinetic temperature: ——, $T = 300$ °K; -----, $T = 500$ °K. ——·——, curve given by Fisher (private communication) for $T_v^0(N_2) = 2200$ °K, $T_v^0(CO) = 300$ °K, $T = 400$ °K. ○, present experimental points ($T_v^0(N_2) \simeq 2200$ °K) $T = 400$ °K.

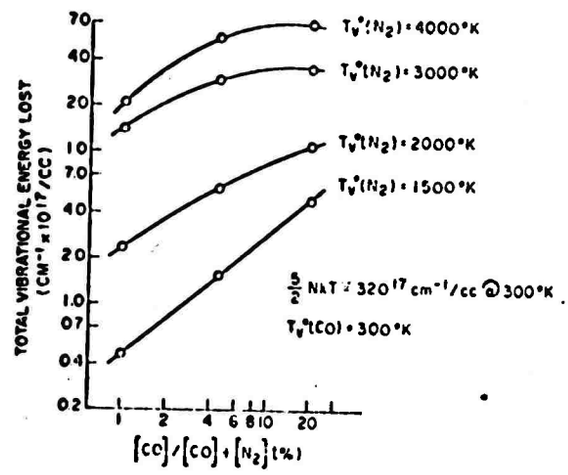

Fig. 15b. Vibrational energy lost into rotational and kinetic energies from initial vibrational distribution to steady state due to nonresonant vibrational exchange processes as a function of composition for N_2 and CO mixtures at different initial N_2 vibrational temperatures and a kinetic temperature of 300°K. The points shown are calculated.

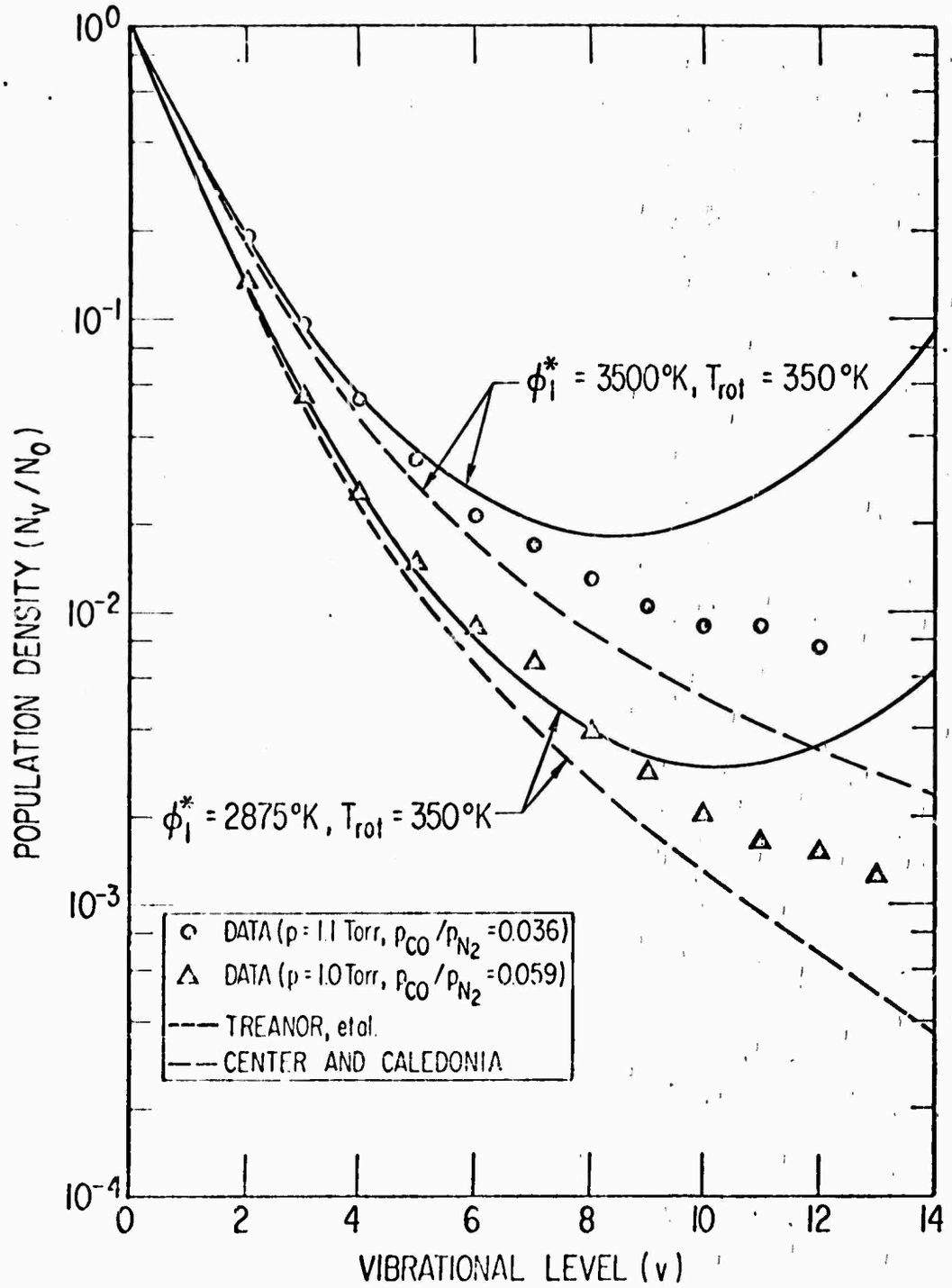

Fig. 16. Steady-State CO Population Density

CO LASER TIME HISTORY

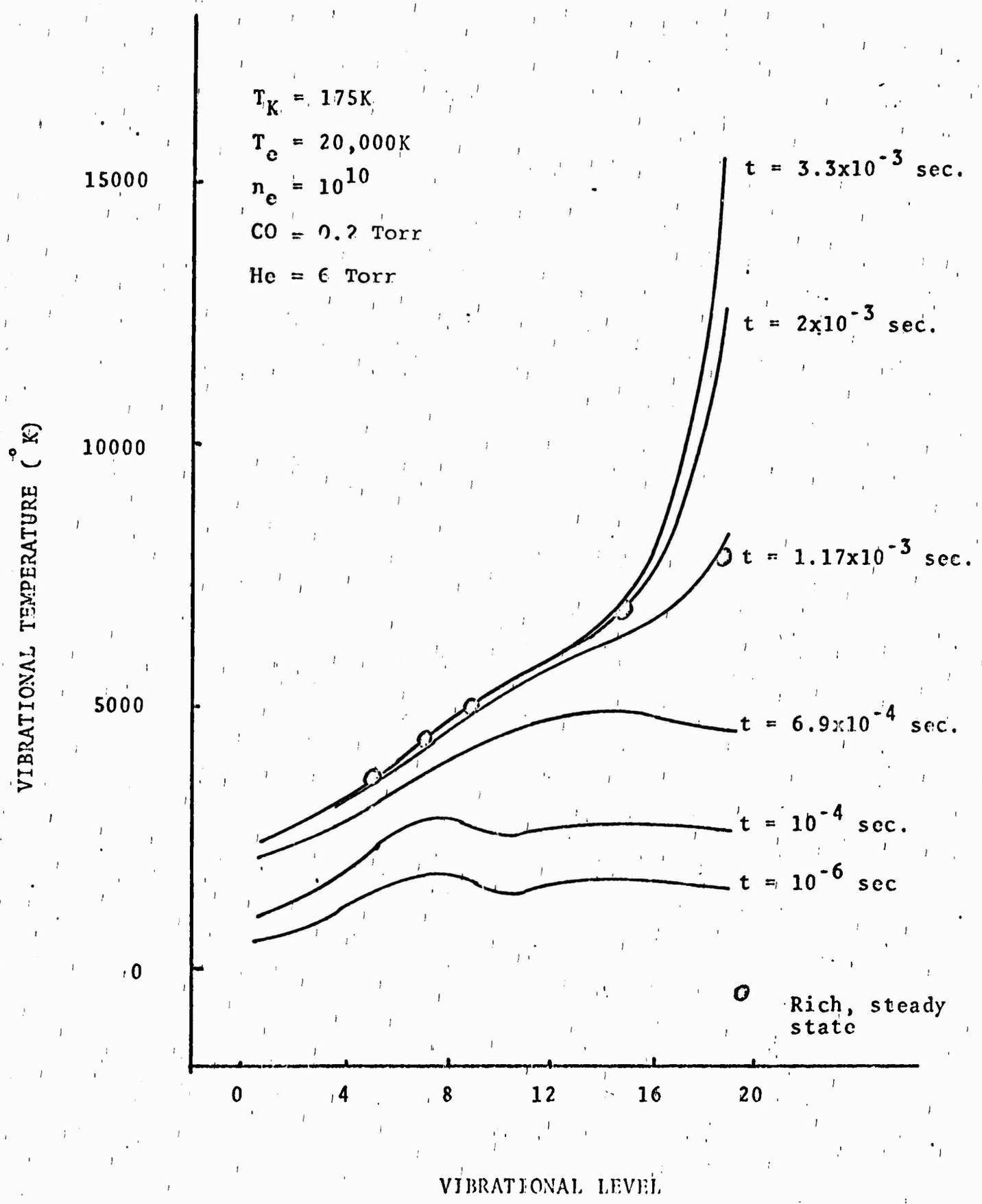

References

1. E. Fisher and R. Kummler, J. Chem. Phys. 49, 1075, (1968).
2. R. Kummler and M. Bortner, Proc. AMRAC Society, 26, (1969).
3. T. Keneshea, A.F.C.R.L. Report 670221, No. 263, April, 1967.
4. J. W. Rich, "Kinetic Modeling of the High Power CO Laser", to be published, Applied Optics, 1971, preprint.
5. M. Mann, M. Blaumik, and W. Lacina, Applied Physics Letters 16, 430 (1970).
6. M. Blaumik, Applied Physics Letters 17, 188 (1970).
7. C. Freed, private communication, by H. Haus Lincoln Labs, 1971.
8. M. Bortner and R. Kummler, Chapter 19, DASA Reaction Rate Handbook, GE TEMPO, Santa Barbara, 1969.
9. G. Shulz, Phys. Rev. 135A, A 988, (1964).
10. B. Moiseiwitsch and S. Smith, Rev. Mod. Phys. 40, 238 (1968).
11. G. Abraham and E. Fisher, RIES Report, (1971).
12. W. Nighan, Phys. Rev. A 1989, (1970).
13. C. Zener, Proc. Roy. Soc. (London) 140, 660 (1933); 137, 696 (1932).
14. E. Bauer, E. Fisher, F. Gilmore, J. Chem. Phys. 51, 4173, (1969).
15. E. Fisher, unpublished work.
16. R. Kummler and M. Bortner, to be published.
17. G. Karl, P. Kruus, and J. C. Polanyi, J. Chem. Phys. 46, 224 (1967).

18. C. Treanon, J. W. Rich, and R. G. Rehm, J. Chem. Phys. 48, 1798 (1968).

19. N. LeGay Sommaire and F. LeGay, Canad. J. Phys. 48, 1966, (1970).

20. J. Rich, private communication, 1970.

21. K. Horn, P. Othergin and A. F. Report No. SAMSO TR 71-4, December 15, 1970.

22. J. Teare, R. Taylor, and C. von Rosenberg, Jr., Nature 225, 240, (1970).

Appendix III

THE VIBRATIONAL EXCITATION OF CO BY COLLISION WITH HELIUM *

R. MARRIOTT
Research Institute for Engineering Sciences
Wayne State University, Detroit, Michigan, U.S.A.

Inelastic processes involving the vibrational excitation of molecules by collision with inert gases are of particular relevance to the study of gas laser phenomena. In this paper cross sections for the vibrational excitation of CO by He impact are calculated, using a computer code previously applied to the case of CO-CO collisions(1).

The code is based upon a close coupling analysis of the collision system. Rotational states of the target and internal structure of the impacting particle are neglected. The molecular wave function is assumed to be separable into electronic, rotational and vibrational components. The scattering potential is similarly assumed to be separable in terms of the vibrational and intermolecular coordinates and to be spherically symmetric. An empirical potential function is subsequently substituted for the intermolecular component.

To this approximation the radial partial wave equations are solved numerically with coupling retained between any specified number of molecular states. Total cross sections are obtained by graphical integration over all significant partial waves.

Previous calculations have found the Lennard-Jones function $4\varepsilon\left((\sigma/r)^{12}-(\sigma/r)^{6}\right)$ to give a satisfactory representation of the scattering potential. The parametric values required for the CO-He system have been tabulated by Hirschfelder et al.(2): $\varepsilon = 9.5\times10^{-5}$(a.u.); $\sigma = 5.93(a_0)$.

The remaining parameters required as data for the code are the oscillator reduced mass (1.26×10^{4}a.u.), the level separation for CO vibrational states (0.266 eV) and the collision reduced mass (6.43×10^{3}a.u.).

Total cross sections for the excitation of CO from the ground to the first vibrational state resulting from the use of the Lennard-Jones potential (LJ) are shown in table 1. Coupling between up to four vibrational states was retained. An indication of the numerical accuracy is given by the requirement for detailed balance which held through to three significant figures.

* Work supported by U.S. Army Research Office - Durham, under Contract No. DAHC04-70-C-0022.

While there are no direct measurements of these cross sections for comparison with the calculated values, they can be used(1) to determine the vibrational relaxation time of CO in He, for which experimental data is available(3).

Assuming only nearest neighbor transitions to be important the relaxation time can be written: $\tau = 1/(\gamma_{10}-\gamma_{01})$ at.sec. where the required rate coefficient is given by

$$\gamma_{01} = 4(10)^{11}(MT)^{-\frac{1}{2}}\int_0^\infty Q_{01}(E)(E/kT)e^{-E/kT}d(E/kT)$$

M a.u. being the collision reduced mass, T °K the gas temperature and $Q_{01}(E)$ is the excitation cross section for the 0→1 transition at a collision energy of E in units of (πa_0^2).

The theoretical relaxation times obtained in this way are shown in figure 1 in comparison with the experimental values of Hooker and Millikan(3). It is immediately apparent that theory is consistently less than experiment by a factor of fifty, indicating that the cross sections are too large by the same amount. This in turn implies that the Lennard-Jones repulsive core, which dominates the excitation process, is too strong.

The scattering studies by Amdur et al.(4,5) of a number of gas molecule potentials indicate that the repulsive part of the interaction between CO and the inert gases behaves as r^{-7} rather than r^{-12}.

Although the CO-He interaction has not been measured directly, data is given on the N_2-He system and it is shown that the CO and N_2 interactions are very similar.

On this basis we estimate the repulsive interaction for CO-He to be $232/r^7$ (a.u.) for separations $3 < r(a_0) < 4.3$. For the long range part the Lennard-Jones potential is assumed still valid and the two functions are smoothly joined over a small region by the common tangent:

$V(r) = .04739-.009158r$ for $4.53 < r(a_0) < 4.84$.

Use of this soft core (SC) potential reduces the strength of the coupling between vibrational states by about a factor of two. Representative values of the SC cross sections are shown in table 1. Coupling has been retained between up to six vibrational states.

Recalculation of the vibrational relaxation time on the basis of these cross sections leads to the third curve shown in figure 1. The theoretical results are now within a factor of three of experiment, except at temperatures below 300 °K where there is a sharp decrease in the temperature dependence of the calculated relaxation time.

Table 1

Cross sections for the vibrational excitation of CO by He.

Potential	LJ	SC	SC	SC
Collision * energy (eV)	Excitation cross sections (πa_0^2) Q_{01}	Q_{01}	Q_{02}	Q_{12}
0.266	0.0^{**}	0.00	----	----
0.600	1.6^{-2}	1.00^{-3}	0.77^{-9}	6.72^{-6}
1.000	2.4^{-1}	1.28^{-2}	2.60^{-6}	4.40^{-3}
1.500	9.7^{-1}	1.13^{-1}	1.66^{-4}	2.82^{-2}
2.000	1.9	4.06^{-1}	1.89^{-3}	8.68^{-2}
2.500	2.6	8.72^{-1}	8.58^{-3}	1.64^{-1}

* Collision energy relative to the ground state.

** Superscript indicates power of 10 by which number must be multiplied.

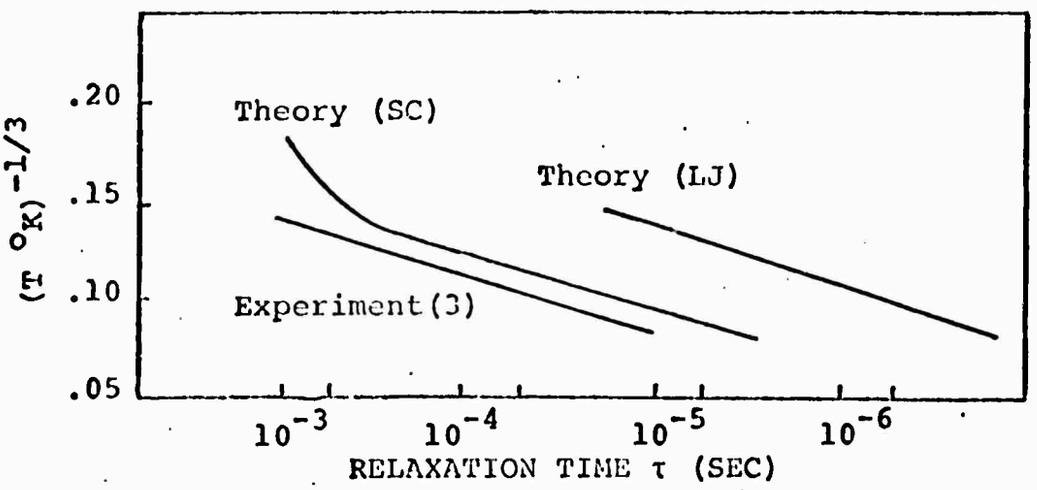

Fig. 1 Vibrational relaxation of CO in He at one atmosphere.

References

(1) F.A.Gianturco and R.Marriott, J. Phys. B 2 (1969) 1332.

(2) J.O.Hirschfelder, F.C.Curtis and R.B.Bird, "Molecular Theory of Gases and Liquids," (New York: John Wiley, 1954)

(3) W.J.Hooker and R.C.Millikan, J. Chem. Phys. 38 (1963) 214.

(4) I.Amdur, E.A.Mason and J.E.Jordan, J. Chem. Phys. 27 (1957) 527.

(5) J.E.Jordan, S.O.Colgate, I.Amdur and E.A.Mason, J. Chem. Phys. 52 (1970) 1143.

PUBLICATIONS, REPORTS and PAPERS

"Vibration-Electronic Coupling in the Quenching of Electronicallu Excited Alkali Atoms by Nitrogen," E.R. Fisher and G.K. Smith, RIES Report No. 70-10 (accepted for publication, Applied Optics Supplement, 1971).

"Fundamental Molecular Processes in Carbon Monoxide Laser Systems," E.R. Fisher and R.H. Kummler, invited paper presented at the Conference on Laser Physics, Sun Valley, Idaho, March 1 - 3, 1971.

"Recent Developments in Solid State Lasers," A.J. Glass, invited paper presented at the American Physical Society Meeting, Washington, D.C., April 26-30, 1970.

"The Vibrational Excitation of CO by Collision with Helium," R. Marriott (accepted for presentation at the VIIth International Conference on the Physics of Electronic and Atomic Collisions, to be held in Amsterdam, The Netherlands, July, 1971).

PARTICIPATING PERSONNEL

Dr. A.J. Glass, Professor of Electrical Engineering, Wayne State University, Detroit, Michigan (Principal Investigator).

Dr. R. Marriott, Professor of Chemical Engineering, Wayne State University, Detroit, Michigan.

Dr. E.R. Fisher, Associate Professor, Chemical Engineering, Wayne State University, Detroit, Michigan.

Dr. J.B. Atkinson, Research Associate (joint appointment with University of Windsor, Canada).

Dr. L. Takacs, Research Associate.

G. Abraham, B.S., Chemical Engineering, Wayne State University (graduate student).